

## Curvature elasticity of thin films

S. A. SAFRAN

Department of Materials and Interfaces, Weizmann Institute of Science, Rehovot  
76100, Israel

[Received 23 December 1996 and accepted 24 December 1997]

### Abstract

A tutorial review of the theory of curvature elasticity of thin films is presented with an emphasis on the physical origins of the bending energy. We begin with a discussion of surface curvature and focus on the role of special surfaces of curvature to show how such surfaces can be defined to eliminate either the coupling of the compressibility and bending terms (neutral surface) or the saddle-splay (Gaussian curvature) modulus. Next, we consider phenomenological models for curvature elasticity and discuss the coupling of the curvature degrees of freedom with other properties of the system such as the packing area and the number of molecules at the interface. The pressure distribution in the film is related to the bending moduli. We then connect the elastic moduli to the physical properties of both solid and liquid thin films with a detailed discussion of the role of solid elasticity (including defects), electrostatic interactions (applicable to polar head groups and chain packing (using a block copolymer model of amphiphilic molecules)). Finally, we demonstrate the effects of fluctuations and inhomogeneities in these systems in a discussion of the role of thermal undulations in renormalizing the bending moduli and of mixtures of amphiphiles of different chain lengths in fluid films. The article is concluded with a brief review of experimental characterizations of curvature elasticity in self-assembling systems.

### Contents

PAGE

1. Introduction	396
2. Curvature: mathematical definitions	399
2.1. Surfaces and curvatures	399
2.2. Invariants of the curvature tensor: mean and Gaussian curvatures	400
2.3. Parallel surfaces	402
3. Phenomenological theory of curvature elasticity	403
3.1. Thermodynamic degrees of freedom in self-assembly	403
3.2. Bending and area changes in membranes and thin films	404
3.3. Neutral surface; surface of vanishing Gaussian modulus	406
3.4. Curvature energy	407
3.5. Thermodynamics of self-assembling fluid interfaces	408
3.5.1. Self-assembly in solution	408
3.5.2. Free energy of self-assembling interfaces	410
3.5.3. Free-energy minimization; effective modulus	412
3.6. Pressure and bending	416
3.6.1. Work of deformation	416
3.6.2. Bending moduli	418
4. Curvature energy of solid thin films	420
4.1. Motivation	420
4.2. Coherent–incoherent bending of solid thin films	421
4.3. Bending with dislocations	423

4.4. Dislocations	425
4.5. Bending of anisotropic solid films	427
5. Microscopic models	429
5.1. Ball-and-spring models	429
5.2. Charged head-group contributions to curvature elasticity	431
5.2.1. Charged surfaces and counterions	431
5.2.2. Bending of charged layers	434
5.3. Chain contributions to curvature elasticity	436
5.3.1. Melt brush	437
5.3.2. Swollen chains at an interface	438
6. Role of thermal fluctuations and inhomogeneities	440
6.1. Thermal fluctuations of thin films	440
6.2. Amphiphilic mixtures: interactions and chain mixing	442
7. Experimental measurements of curvature elasticity	443
7.1. Experimental estimates of bending moduli	443
7.2. Emulsification failure: drop size and interfacial tension	444
7.3. Electrostatic contributions to the bending modulus	445
Acknowledgments	446
References	446

## 1. Introduction

Recent interest in the development of nanoscale materials has focused attention on the morphology of thin films with unusual topologies. The self-assembly [1, 2] of fluid thin films is a challenging area of both experimental and theoretical research with implications for both chemical technology and biology. The fascinating and useful variety of shapes, sizes and forms found in these systems which include micelles (amphiphilic<sup>†</sup> aggregates in a single solvent such as water), vesicles (closed bilayer structures formed by amphiphiles in a single solvent) [3] and microemulsions (three-component solutions of water, oil and surfactant) [4] is related to the flexibility of the amphiphilic interface<sup>†</sup> (figure 1) to change its geometry. In many of (but not all) these systems the domain sizes are much larger than molecular scales and one can speak of an interfacial film. It is precisely these systems that give rise to the most striking macroscopic behaviour and many of their properties can be rationalized and predicted in terms of the curvature elastic behaviour of the interface. In the realm of solid-state materials, recent attention has focused on the curved structures in 'fullerenes' which consist of single layers or nested planes of carbon and other layered compounds, where the layers may be organized into nearly spherical (for a review see [5]), cylindrical [6] or even saddle-shaped [7] structures.

If the films were constrained to lie in a plane, the only relevant energy would be the compression of the molecules, that is changes in the average area per molecule in the film, or in the case of a solid film the shear. However, since the membrane can also deform in the normal direction (out of the plane), there is an additional set of 'modes' describing the conformations of the film. These out-of-plane deformations are known as bending or curvature modes and the free energy associated with such modes is known as the curvature free energy. For a membrane with finite thickness,

---

<sup>†</sup> Amphiphilic molecules, examples of which include surfactant (soap-like) and lipid molecules, contain polar regions which prefer high dielectric constant (polar) solvents such as water and hydrocarbon regions which prefer non-polar solvents such as oil. They typically self-assemble in monolayers at water-oil interfaces or into bilayers in a single solvent.

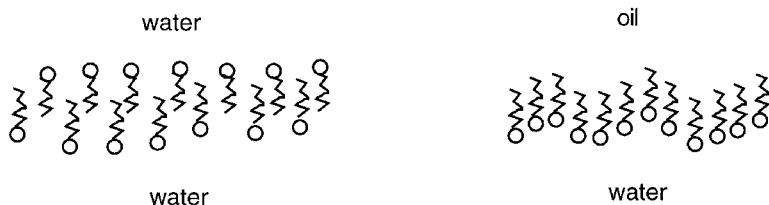


Figure 1. Monolayer and bilayer membranes composed of amphiphiles at the interfaces between two different solvents (oil–water in the case of the monolayer) or the same solvent (water in the case of the bilayer).

we denote as pure curvature deformations those perturbations of the membrane that do not change the overall membrane volume, but where there may be local stretching and compression of different parts of the film. While a general deformation of the membrane involves a change in both volume and curvature, we shall see that the lowest-energy deformations usually involve only the curvature. In most systems, changing the average density of the membrane is a higher-energy process and hence is less important when effects involving the thermal behaviour of the membrane are considered. The curvature energy is non-extensive and thus has subtle and fascinating implications for the structure of materials. This non-extensivity is demonstrated by the fact that the energy to bend a thin film (which is preferentially flat) into a sphere is independent of the sphere size.

In this tutorial review, we focus on the meaning and microscopic origins of curvature elasticity in the limit of gently curved interfaces, situations where the radius of curvature is much larger than the thickness of the interface. Much of the recent work on self-assembling or even polymerized membranes has focused on the statistical mechanical behaviour of the system with particular emphasis on the relationship between the curvature energy and the long-wavelength thermal fluctuations of the structure. However, it is of fundamental interest to understand the origin of the curvature elastic energy which, in almost all these cases, provides the restoring force against thermal undulations. In addition, as mentioned previously, there is a wide variety of materials whose thin-film properties depend on curvature elasticity and it is of interest to outline how the different properties of the underlying material influence the bending moduli. In some cases, these moduli are entropic in origin (e.g. in the case of charged membranes with counterions in solution or in the case of polymeric chains) and what is thought of as a ‘microscopic’ picture in reality results from the effects of thermal fluctuations.

After defining the curvature tensor and the mean curvature  $H$  and Gaussian curvature  $K$  of a surface, we begin with an outline of a phenomenological theory of curvature elasticity in thin films to motivate the classical expression [8] for the bending or curvature free energy  $f_b$  per unit area:

$$f_c = \frac{1}{2}k(H - c_0)^2 + \bar{k}K. \quad (1.1)$$

The properties of the interface determine the bending moduli  $k$  (known as the bending or curvature modulus) and  $\bar{k}$  (known as the saddle-splay or Gaussian curvature modulus) as well as the spontaneous curvature  $c_0$ . This expression for  $f_b$ , which is essentially an expansion of the free energy for small curvatures, is correct in the limit of radii of curvatures that are large compared with the thickness of the film.

A treatment of the bending energy of thick films (compared with their radii of curvature) requires a more detailed treatment of each particular case; the situation discussed here of thin film bending is particularly useful precisely because of the universality of the general form of the energy. The first term in  $f_b$  represents the change in energy if the average curvature of the film deviates from the spontaneous curvature which is a property of a given film in a particular environment. The second term represents the part of the energy which depends on the Gaussian curvature, and hence on the topology of the film<sup>†</sup>.

We begin the review by discussing a general expression for the free energy of a mathematically thin surface or interface; all the physics behind the curvature energy is lumped into phenomenological coefficients in an expansion of the free energy as a function of the area per molecule and the curvature of the interface. We show how a certain choice of the surface of curvature can decouple terms in the energy which involve the changes in area per molecule (compressibility) and the curvature of the surface; this is commonly known as the choice of a neutral surface. In addition, we show how a different choice for the surface of curvature can result in the vanishing of one of the curvature moduli (the Gaussian or saddle-splay modulus); this is somewhat less known but has been discussed in the past in the context of specific microscopic models [9]. We tailor this discussion to the case of self-assembly of amphiphilic molecules and consider the possibility of interfaces with a variable number of molecules; this is the case for amphiphilic interfaces that are in thermodynamic equilibrium with the same molecules in dilute solution. Here, the system has an additional degree of freedom since the molecules which self-assemble can leave the interface and go into solution when the interface is deformed. We show how this can dramatically reduce the curvature moduli in the very dilute regime where the self-assembly process first begins; at higher concentrations, we show that the bending moduli are almost independent of amphiphile concentration and can be related to those of an almost isolated, mechanical system.

In order to relate the phenomenological model to the physics of the interface it is necessary to consider the energetics of a surface of finite thickness and to relate the deformation energy to the internal stresses or pressure. We obtain expressions for the curvature moduli in terms of the moments of the internal pressure distribution and their derivatives. While the pressure expansion applies to both solid and liquid thin films, solid materials have an additional restoring force which arises from their shear modulus. We consider the general case of an anisotropic material which is relevant to the layered solids that form fullerene-type structures. In these materials, the interplanar bonding arises from van der Waals forces and is much weaker than the in-plane covalent bonds. In addition, solids have the freedom to form defects such as dislocations and their role in lowering the bending moduli of solid thin films is discussed and applied to fullerene-type materials.

To apply the formulae which relate the curvature moduli to the pressure distribution, one must consider specific physical situations; we discuss the contributions to the bending moduli from charged polar head groups and from flexible

---

<sup>†</sup> The Gauss-Bonnet theorem relates the surface integral of the Gaussian curvature to the topology of the surface such as the number of holes and handles:  $\int dS K = 4\pi(1 - g)$ , where  $g$  is the Euler characteristic of the surface, for example,  $g = 0$  for a spherical topology and  $g = 1$  for a simple toroidal topology.

polymer-like chains. These are the primary contributions in the case of amphiphilic molecules; in both cases, the restoring forces are related to the changes in the entropy of the molecular configurations upon bending. Finally, we demonstrate the effects of fluctuations and inhomogeneities in these systems in a discussion of the role of thermal undulations in renormalizing the bending moduli and of mixtures of amphiphiles of different chain lengths in fluid films. While most of the article treats the local bending free energy of an amphiphilic interface without thermal fluctuations, the undulations are of particular importance in determining the large-scale structure and phase behaviour of amphiphilic systems. We show how long-wavelength fluctuations (the entropic degrees of freedom) soften the effective bending modulus of the interface. In mixtures, the degrees of freedom associated with the mixing also can make the bending modulus lower than one would expect. The article concludes with a brief review of experimental characterizations of curvature elasticity in self-assembling systems and some open questions.

## 2. Curvature: mathematical definitions

In this section, we define the mean and Gaussian curvatures of a mathematically, infinitely thin surface. We point out that the mean curvature  $H$  and Gaussian curvature  $K$  are invariants of the surface and therefore independent of the particular coordinate system or representation of the surface.

### 2.1. Surfaces and curvatures

Surfaces can be described firstly by the parametric form  $x = f(u, v)$ ,  $y = g(u, v)$  and  $z = h(u, v)$ , which determine a vector  $\mathbf{r}(u, v)$  which locates (in the three-dimensional ‘laboratory’ frame) points on the surface, or secondly by the implicit form  $F(x, y, z) = 0$ . A simple example of the parametric form is where  $u$  and  $v$  are equal to  $x$  and  $y$  respectively and the ‘height’  $z = h(u, v) = h(x, y)$ . This is called the *Monge parametrization* of a surface and the position of the surface (see figure 2) is given by

$$\mathbf{r} = (u, v, h(u, v)) = (x, y, h(x, y)). \quad (2.1)$$

On the surface one defines the *two* tangent vectors  $\mathbf{r}_u = \partial \mathbf{r} / \partial u$  and  $\mathbf{r}_v = \partial \mathbf{r} / \partial v$ . These vectors are not necessarily unit vectors, nor are they necessarily orthogonal. The two vectors define a tangent plane. The equation of the plane is given by  $\mathbf{r} \cdot \hat{\mathbf{n}} = 0$  where  $\hat{\mathbf{n}}$  is the normal to the surface at ‘positions’  $(u, v)$ . The normal is given by the cross product:

$$\hat{\mathbf{n}} = \frac{\mathbf{r}_u \times \mathbf{r}_v}{|\mathbf{r}_u \times \mathbf{r}_v|}. \quad (2.2)$$

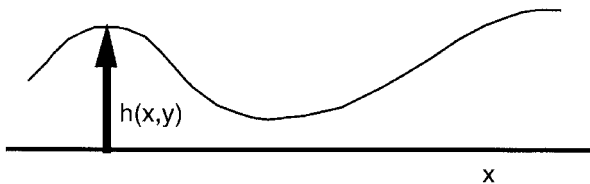


Figure 2. A surface in the Monge representation where the height is denoted by  $h(x, y)$ .

The implicit definition of a surface,  $F(x, y, z) = 0$ , gives in the Monge representation  $F(x, y, z) = z - h(x, y) = 0$ . For the general implicit form, one obtains the normal by realizing that on the surface, where  $F$  is a constant, the total derivative of  $F$  is zero:

$$dF = d\mathbf{r} \cdot \nabla F = 0, \quad (2.3)$$

where  $d\mathbf{r}$  is a vector connecting two points in the surface. Since  $d\mathbf{r}$  is a vector that is tangent to a certain direction in the surface, equation (2.3) indicates that  $\nabla F$  is orthogonal to this tangent; the normal vector is thus parallel to  $\nabla F$  (with  $F$  evaluated on the surface). The unit normal is thus given by

$$\hat{\mathbf{n}} = \frac{\nabla F}{|\nabla F|}. \quad (2.4)$$

It is well known that the curvature of a linear object is given by the change in the tangent as one moves along the arc length of the curve. Similarly, the curvature for a curve on the surface can be derived from the implicit form of the surface,  $F(x, y, z) = 0$  by considering the change in the normal vector defined from equation (2.4) as one proceeds along the surface. Thus, if one moves along the surface a distance  $d\mathbf{r}$ , the normal  $\hat{\mathbf{n}}$  changes by an amount

$$d\hat{\mathbf{n}} = d\mathbf{r} \cdot \mathbf{Q}, \quad (2.5)$$

where  $\mathbf{Q}$  is a tensor whose elements in Cartesian coordinates are given by differentiating equation (2.4):

$$Q_{ij} = \frac{1}{Y} \left( F_{ij} - \frac{F_i Y_j}{Y} \right), \quad (2.6)$$

where  $Y = |\nabla F|$  and  $F_i = \partial F / \partial r_i$ , where  $\mathbf{r} = (x, y, z)$ , with a similar notation for  $Y_i$ . By taking the dot product of equation (2.5) with  $d\mathbf{r}$ , one obtains an expression for the curvature along a given curvilinear direction that is proportional to the trace of the tensor  $\mathbf{Q}$ . Thus, the curvature is associated with the change in the normal as one moves along the surface. Since both the normal and the direction along the surface are vectors, the curvature is, in general, a tensor quantity.

## 2.2. Invariants of the curvature tensor: mean and Gaussian curvatures

It is useful to describe the curvature tensor by its invariants, since these quantities do not change if one rotates the coordinate system used to describe the surface; the invariants are intrinsic properties of the surface. For the implicit representation of the surface,  $F(x, y, z) = 0$ , the curvature along a general direction is related to the tensor  $\mathbf{Q}$  defined in equation (2.6). In three dimensions,  $\mathbf{Q}$  is a  $3 \times 3$  matrix with three eigenvalues. One can show by explicit calculation using equation (2.6) with  $Y = |\nabla F|$  that the determinant of  $\mathbf{Q}$  and one eigenvalue are zero. The remaining two eigenvalues are the two principal curvatures of the surface; these can be calculated for any  $F$  directly from  $\mathbf{Q}$ .

The three-dimensional tensor  $\mathbf{Q}$  has three invariants under similarity transformations (which include rotations): its trace, the sum of the principal minors (i.e., the three minors formed by crossing out the rows and columns of the diagonal elements), and its determinant (for a proof see [2]). Explicit calculation shows that the determinant of  $\mathbf{Q}$  is zero. Two of the eigenvalues of  $\mathbf{Q}$  have dimensions of an inverse length and are known as the principal curvatures (one eigenvalue is zero). The

eigenvectors corresponding to the non-zero eigenvalues are known as the principal directions of the surface; along these directions, the curvature tensor is diagonal. The trace, which is the sum of the eigenvalues (i.e., principal curvatures), is twice the mean curvature  $H$ ; both quantities have the dimensions of an inverse length. The other invariant of the tensor  $\mathbf{Q}$  is the sum of the principal minors, which has the dimensions of an inverse length squared and is termed the Gaussian curvature  $K$ , which is equal to the product of the two principal curvatures (eigenvalues of  $\mathbf{Q}$ ). Using equation (2.6) we find an expression for the mean curvature:

$$H = \frac{1}{2Y^3} [F_{xx}(F_y^2 + F_z^2) - 2F_x F_y F_{xy} + \text{Perm}], \quad (2.7)$$

where the term Perm indicates that one should consider two additional permutations of each term—one where  $(x, y, z) \rightarrow (z, x, y)$  and another with  $(x, y, z) \rightarrow (y, z, x)$ —and where

$$Y = (F_x^2 + F_y^2 + F_z^2)^{1/2}. \quad (2.8)$$

The Gaussian curvature is given by

$$K = \frac{1}{Y^4} [F_{xx}F_{yy}F_z^2 - F_{xy}^2F_z^2 + 2F_{xz}F_x(F_yF_{yz} - F_zF_{yy}) + \text{Perm}]. \quad (2.9)$$

In the case where  $F$  is described by the Monge parametrization  $F = z - h(x, y)$ , these expressions simplify considerably and one obtains:

$$H = \frac{(1 + h_x^2)h_{yy} + (1 + h_y^2)h_{xx} - 2h_x h_y h_{xy}}{2[(1 + h_x^2 + h_y^2)]^{3/2}}, \quad (2.10)$$

$$K = \frac{h_{xx}h_{yy} - h_{xy}^2}{(1 + h_x^2 + h_y^2)^2}. \quad (2.11)$$

In the limit of a nearly flat surface,  $h_x \ll 1$ ,  $h_y \ll 1$ ; the mean and Gaussian curvatures can be approximately written as

$$H \approx \frac{1}{2}(h_{xx} + h_{yy}), \quad (2.12)$$

$$K \approx h_{xx}h_{yy} - h_{xy}^2. \quad (2.13)$$

Another way to think about surface curvature is in terms of the parametric representation of the surface  $\mathbf{r}(u, v)$  with components:  $x = f(u, v)$ ,  $y = g(u, v)$ , and  $z = h(u, v)$ . The (linear) curvature along an arbitrary direction in the surface  $\hat{\mathbf{a}} = l\mathbf{r}_u + m\mathbf{r}_v$ , is a quadratic function of the values of  $l$  and  $m$ . As shown in [2], the curvature  $\kappa$  is

$$\kappa = Ll^2 + 2Mlm + Nm^2, \quad (2.14)$$

where  $L$ ,  $M$  and  $N$  are related to derivatives of the normal with respect to the coordinates  $u$  and  $v$  (see equation (2.2))

$$L = -\hat{\mathbf{n}}_u \cdot \mathbf{r}_{uu}, \quad M = -\hat{\mathbf{n}}_v \cdot \mathbf{r}_{uv} = -\hat{\mathbf{n}}_u \cdot \mathbf{r}_{vu}, \quad N = -\hat{\mathbf{n}}_v \cdot \mathbf{r}_{vv}. \quad (2.15)$$

Diagonalizing this quadratic form of  $\kappa$ , subject to the constraint that  $\hat{\mathbf{a}}$  is a unit vector, is mathematically equivalent to the minimization–maximization of  $\kappa$ . Thus,

the extremal curvatures,  $\kappa_a$  and  $\kappa_b$  are determined by the extremal values of  $l$  and  $m$ , which we denote as  $l^*$  and  $m^*$ . For directions on the surface close to these extremal values, the expansion of the curvature as a function of  $l - l^*$  and  $m - m^*$  has no linear terms since  $l^*$  and  $m^*$  are extremal; in this sense, the local curvature is a diagonalized quadratic form. The mean curvature is the average  $H = \frac{1}{2}(\kappa_a + \kappa_b)$  while the Gaussian curvature is the product  $K = \kappa_a \kappa_b$  and one finds that

$$H = \frac{EN + GL - 2FM}{2(EG - F^2)}, \quad (2.16)$$

$$K = \frac{LN - M^2}{EG - F^2}, \quad (2.17)$$

where

$$E = \mathbf{r}_u^2, \quad F = \mathbf{r}_u \cdot \mathbf{r}_v, \quad G = \mathbf{r}_v^2. \quad (2.18)$$

### 2.3. Parallel surfaces

Consider a locally flat surface (e.g. in the Monge gauge  $|\nabla h| \ll 1$ ) and imagine translating that surface along the normal direction, a distance  $\delta$  to obtain a parallel surface (figure 3) whose location is given by

$$\mathbf{r}' = \mathbf{r}(u, v) + \hat{\mathbf{n}}\delta. \quad (2.19)$$

The relation of the area element  $dA'$ , mean curvature  $H'$  and Gaussian curvature  $K'$  on the parallel surface compared with the original surface with area  $dA$ , and curvatures  $H$  and  $K$  is given by

$$dA' = dA(1 + 2H\delta + K\delta^2), \quad (2.20)$$

$$H' = \frac{H + K\delta}{1 + 2H\delta + K\delta^2}, \quad (2.21)$$

$$K' = \frac{K}{1 + 2H\delta + K\delta^2}, \quad (2.22)$$

and the normals are of course equal to within a sign. These relations are important in understanding the properties of surfaces of finite thickness. (The proof is straightforward, but lengthy and simplifies if one chooses the lines of curvature as parametric curves.)

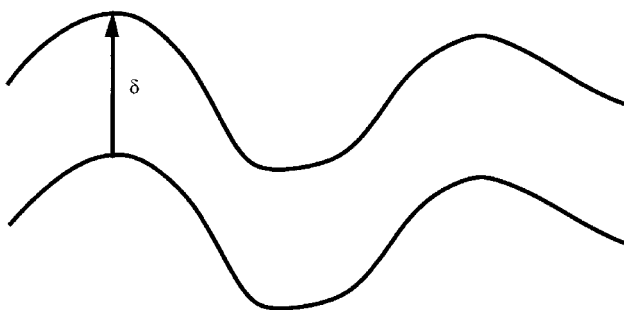


Figure 3. Schematic drawing of two parallel surfaces separated by a distance  $\delta$  along the normal.



### 3. Phenomenological theory of curvature elasticity

Although solid thin films as well as fluid membranes can be composed of many different types of chemical and molecular species, their behaviour (equilibrium shapes as well as their thermal fluctuations) can be understood from a unified point of view that considers the free-energy cost of deformations of the membrane. We begin with an enumeration of the thermodynamic degrees of freedom that exist in self-assembling systems: solubility of the amphiphilic molecules, the sizes and shapes of the interfaces formed, the number of interfaces that exist, and the area per molecule at these interfaces. We point out the conditions under which the tensions of the interfaces in the system can be considered to be zero and when these tensions are finite. Next, we discuss the free energy of a single thin film and consider, in addition to the curvature, the area per molecule as a degree of freedom which can be adjusted by the system to minimize the energy. The thickness of the film plays no explicit role in this initial discussion; it enters indirectly in the phenomenological constants used to write the energy as a function of area per molecule and curvature. We show firstly that the freedom that the system has to adjust the area per molecule upon bending, reduces the bending modulus and secondly that the surface of curvature can be chosen either to decouple changes in area from those in curvature (this is the so-called neutral surface) or to result in a zero value for the Gaussian curvature modulus.

Another relevant degree of freedom in self-assembling membranes is the finite solubility of the molecules of the film in the solution; for a system in equilibrium with amphiphilic molecules in solution, the membrane can sometimes respond to bending by moving molecules from the film into the solution (or into the vapour that coexists with a solid film). We show in section 3.5 how this effect can also result in a reduced bending modulus, but only in a small range of amphiphile volume fractions where the films have a free energy that is comparable with that of the amphiphiles in solution (critical aggregation concentration).

In order to obtain more physical insight into the origin of the bending moduli, it is necessary to consider explicitly the effects of bending a film of finite thickness. In the case of solid films, one can derive the bending elasticity by considering the elastic energy explicitly; this is done in section 4. For a fluid film, one can relate these moduli to the pressure distribution which varies through the thickness of the film and in section 3.6 we show that a completely isotropic fluid (or gas) film has no response to bending. The physics of various types of pressure distributions are discussed in section 5, which considers the electrostatic and chain contributions to the bending moduli for particular systems.

#### 3.1. *Thermodynamic degrees of freedom in self-assembly*

The theoretical description of the free energy and associated constraints in self-assembling systems can be subtle. Although it is commonly stated that self-assembling membranes have zero interfacial tensions, this is rigorously true only in the particular limit of a single membrane whose amphiphilic components are insoluble in the solvent. It is more generally true, however, that self-assembling membranes determine the area  $\Sigma$  per molecule, for packing of the amphiphilic molecules from equilibrium considerations and that the free energy is a minimum when varied with respect to  $\Sigma$ .

Any discussion of the thermodynamic degrees of freedom in self-assembly must consider two cases: firstly soluble amphiphiles (where the membranes formed can

exchange molecules with the amphiphile monomers in solution) and secondly insoluble amphiphiles (where there is no such exchange). In the case of insoluble amphiphiles, the area of the system is determined by the total area of all the membranes in the system. In general, the many membranes or globules that coexist in the solution can have different sizes and shapes and the area per molecule will differ from membrane to membrane; even within a single membrane it can also be a function of the local curvature. The area per molecule can also depend on the entropy of mixing of the membranes or globules in solution and upon their interactions. However, if the interaction energies are small compared with the typical molecular compressibilities and if the membrane radii of curvature are much larger than any molecular size (e.g. the size associated with a typical area per molecule), then, to a good approximation,  $\Sigma$  can be taken to be a constant. In this case, the total area of all the membranes is fixed by the total number of molecules in solution and the area  $\Sigma$  per molecule is determined to zeroth order by minimizing the free area of a flat membrane with respect to  $\Sigma$ ; it is this free-energy derivative (a type of interfacial tension) that is zero in this case. Of course, the number, size and shape of all the membranes in the solution are still degrees of freedom to be considered and the distribution of these degrees of freedom must be found. In a mean-field type of approximation where one considers only one typical membrane or globule size and shape, the free energy can be minimized with respect to these degrees of freedom, provided that one takes into account the conservation constraints.

The case of a single membrane with insoluble amphiphiles is even simpler. Here, the total area is fixed by the total number of molecules; if one neglects curvature or fluctuation corrections to  $\Sigma$ , the derivative of the free energy with respect to  $\Sigma$  is zero. This limiting case, therefore, shows a zero interfacial tension. The situation for the case where the curvature corrections to  $\Sigma$  are explicitly taken into account is discussed in the next section.

When the amphiphilic molecules are soluble in the solution, there is no longer a constraint of fixed total membrane area since the film molecules can exchange with those in solution. The constraint of a fixed total number of amphiphilic molecules (in both the solution and the film) dictates the equality of the chemical potential for the amphiphiles which determines their partitioning in the solution and in the film. This case is discussed in section 3.5. Here we note that, in the approximation where the interactions between membranes and curvature corrections to the packing area  $\Sigma$  can be neglected, the area per molecule is still determined to zeroth order by the minimum of the free energy of the flat film and in that sense there is an approximately zero tension in the system. However, the derivative of the membrane free energy with respect to the membrane area is not zero, instead, it is equal to the chemical potential (divided by  $\Sigma$ ) of the amphiphilic molecules in solution.

Heretofore, we have focused on the degrees of freedom of membranes with no shape fluctuations. When such undulations are important, one must also differentiate between the projected area and the actual area of the membrane. The usual interfacial tension would then refer to changes in the projected area. However, a detailed discussion of these additional degrees of freedom and their conjugate tensions is outside the scope of this article.

### 3.2. *Bending and area changes in membranes and thin films*

Microscopic models of amphiphilic interfaces often tie the interface location to a particular molecular site (e.g. the bond joining the two parts of a block copolymer,

the polar head group in a surfactant). It is therefore useful to describe the energy of a bent film or membrane for a general location of the surface of curvature, since the location of this surface is often dictated by molecular considerations and cannot be arbitrarily assigned when using a particular microscopic model. As mentioned previously, we first consider a single, infinitely thin, surface (whose amphiphilic molecules are insoluble in the solution). The free energy per molecule is a function of both the area  $\Sigma$  per molecule and the curvature. (The membrane thickness enters only indirectly in determining the phenomenological expansion parameters; the explicit dependence of the bending on thickness is described in section 3.6.) To describe the novel large-scale structures observed in these systems and to characterize the low-energy deformations that are most strongly influenced by thermal fluctuations, we consider radii of curvature whose length scales are much larger than molecular sizes.

We write an expansion of the free energy  $f$  per molecule for small curvatures (the dimensionless small parameter is the product of the curvature and the membrane thickness) up to second order. As explained previously, the two invariants of the surface to this order in curvature are the mean curvature  $H$  and the Gaussian curvature  $K$ ; since the free energy of a fluid membrane must be invariant under rotations of the coordinate system,  $f$  is thus a function of  $H$ ,  $H^2$  and  $K$  to the order that we consider. Thus,

$$f(\Sigma, H, K) = f_0(\Sigma) + f_1(\Sigma)H + f_2(\Sigma)H^2 + \bar{f}_2(\Sigma)K, \quad (3.1)$$

where the coefficients of the curvature are, in general, functions of the equilibrium area per molecule, which itself may depend on curvature. The free energy of the flat film is  $f_0$  and  $f_1$ ,  $f_2$  and  $\bar{f}_2$  are derivatives of the free energy with respect to  $H$ ,  $H^2$  and  $K$  respectively. Since the free energy of the flat layer has a minimum when  $\Sigma = \Sigma_0$ , a change in  $\Sigma$  that is *linear* in curvature contributes a term *quadratic* in curvature to the free energy; the free energy has no term that is linear in  $\Sigma - \Sigma_0$  because  $\partial f_0 / \partial \Sigma_0 = 0$ . We thus expand  $f_0$  to second order and  $f_1$  to first order in  $\Sigma - \Sigma_0$  to find that

$$\begin{aligned} f(\Sigma, H, K) \approx & f_0(\Sigma_0) + \frac{1}{2} f_0''(\Sigma_0)(\Sigma - \Sigma_0)^2 + f_1(\Sigma_0)H \\ & + f_1'(\Sigma_0)(\Sigma - \Sigma_0)H + f_2(\Sigma_0)H^2 + \bar{f}_2(\Sigma_0)K, \end{aligned} \quad (3.2)$$

where

$$f_0''(\Sigma_0) = \left( \frac{\partial^2 f_0}{\partial \Sigma^2} \right)_{\Sigma_0} \quad (3.3)$$

and

$$f_1'(\Sigma_0) = \left( \frac{\partial f_1}{\partial \Sigma} \right)_{\Sigma_0}. \quad (3.4)$$

The terms proportional to  $H^2$  and  $K$  are already of quadratic order in our expansion. Their coefficients need only be kept to lowest order in the expansion of  $\Sigma$  and are therefore given by  $f_2$  and  $\bar{f}_2$  evaluated at  $\Sigma = \Sigma_0$ . Minimizing the free energy to determine the equilibrium area  $\Sigma^*$  per molecule of the *curved* interface we find that

$$\Sigma^* = \Sigma_0 - \left( \frac{f_1'}{f_0''} \right) H. \quad (3.5)$$

Evaluating the free energy at the optimal value of the area  $\Sigma^*$  per molecule we see that  $f$  depends only on  $H$  and  $K$ . This defines the *curvature free energy* via

$$f(\Sigma^*, H, K) = g_0 + g_1 H + g_2 H^2 + \bar{g}_2 K \quad (3.6)$$

where  $g_0 = f_0(\Sigma_0)$ ,  $g_1 = f_1(\Sigma_0)$ ,  $\bar{g}_2 = \bar{f}_2(\Sigma_0)$  and

$$g_2 = f_2(\Sigma_0) - \frac{1}{2} \frac{f_1'^2}{f_0''}. \quad (3.7)$$

Note that the correction term which makes the area per molecule depend on curvature is always negative since  $f_0'' > 0$  by the minimization condition and the stability of the flat layer. Physically, this means that, if the molecules are allowed to adjust their area per molecule depending on the curvature, the monolayer will be less rigid upon bending than if constrained to have a fixed area per molecule. We thus see that there is a term independent of curvature (the flat layer free energy), a term linear in curvature (which must vanish for a symmetric bilayer, but which is present for a monolayer) and a term quadratic in curvature.

### 3.3. Neutral surface; surface of vanishing Gaussian modulus

In the preceding discussion, the area per molecule had a correction term due to curvature. This arose because of a coupling between the stretching and curvature of the surface, that is the term proportional to  $(\Sigma - \Sigma_0)H$  in equation (3.2). This coupling can be eliminated by a shift in the normal direction of the surface of curvature by an amount  $\lambda$  whose magnitude is determined as follows: The curvature on the new interface changes (see the previous discussion of parallel surfaces in section 2.3) according to

$$H' \approx H(1 + 2\lambda H) - \lambda K. \quad (3.8)$$

The higher-order terms as well as the change in the Gaussian curvature are negligible if one keeps the free energy to second order in the curvatures only. The area  $\Sigma'$  per molecule defined with respect to the new interface is related to the area per molecule defined on the original interface by

$$\Sigma' \approx \Sigma(1 - 2\lambda H), \quad (3.9)$$

where we keep terms linear in  $H$  only since the energy (equation (3.2)) depends quadratically on deviations of  $\Sigma$  from its value on the flat interface. Rewriting the bending energy as a function of both  $\Sigma'$  and the curvatures (which have negligible higher-order corrections due to the shift of the interface position), and keeping terms up to order  $H^2$ ,  $(\Sigma - \Sigma_0)^2$  and  $(\Sigma - \Sigma_0)H$ , equation (3.2) becomes

$$\begin{aligned} f(\Sigma', H', K') &\approx f_0(\Sigma_0) + \frac{1}{2} f_0''(\Sigma' - \Sigma_0)^2 + f_1(\Sigma_0)H' \\ &\quad + H'(\Sigma' - \Sigma_0)(f_1' + 2\Sigma_0\lambda f_0'') + [\bar{f}_2(\Sigma_0) + f_1(\Sigma_0)\lambda]K' \\ &\quad + [2f_0''\Sigma_0^2\lambda^2 + 2f_1'\Sigma_0\lambda + f_2(\Sigma_0) - f_1(\Sigma_0)\lambda]H'^2, \end{aligned} \quad (3.10)$$

where the extra terms arise from the change in the interface position.

The neutral surface is obtained by choosing the shift at the interface position,  $\lambda = \lambda_n$ , so that there are no terms in  $f(\Sigma, H, K)$  where the area and curvatures are coupled. From equation (3.10), one sees that this is the case when

$$\lambda_n = -\frac{f_1'}{2\Sigma_0 f_0''}. \quad (3.11)$$

The only dependence of  $\Sigma'$  in the free energy is a term proportional to  $(\Sigma' - \Sigma_0)^2$ , so that at the neutral surface the minimum free energy configuration is given by  $\Sigma' = \Sigma_0$ ; that is there is no change in the area per molecule compared with the flat surface. When the free energy is evaluated at the minimal value of  $\Sigma'$ , only pure bending terms contribute and we find a free energy of the form of equations (3.6) and (3.7), with  $g_1$  and  $\bar{g}_2$  as given previously, but where  $\bar{g}_2$ , the coefficient of  $H'^2$  has several additional contributions (given by the last term of equation (3.10) evaluated with  $\lambda = \lambda_n$ ).

In addition to the neutral surface where the coupling between the area changes and the curvature vanishes we can define another type of special surface [9] where the effective Gaussian curvature modulus vanishes. The value of  $\lambda$  at which this occurs is given by

$$\bar{\lambda} = -\frac{\bar{f}_2(\Sigma_0)}{f_1(\Sigma_0)}. \quad (3.12)$$

Of course, this surface is, in general, not the same as the neutral surface and one can only choose the definition of the surface of curvature once. Thus, one can choose the surface of curvature to lie either on the neutral surface or on the surface where the effective saddle-splay modulus vanishes. In addition, one has to check that the value of  $\lambda$  where the effective Gaussian curvature modulus vanishes is physically meaningful, that is not much larger than the film thickness; otherwise the surface of curvature is too far removed from the actual film. Dimensional analysis shows that  $f_2/f_1$  does indeed have the dimensions of a length which one expects to be proportional to the spontaneous radius  $(1/c_0)$  of curvature. Since the continuum theory is most appropriate when  $1/c_0$  is large compared with a molecular size, one might think that there is never a situation where  $\bar{\lambda}$  is comparable with the film thickness. However, there may arise situations (see equation (5.4)) where the Gaussian curvature modulus itself becomes proportional to the spontaneous curvature and the value of  $\bar{\lambda}$  indeed does become of the order of the film thickness (or smaller) and hence physically meaningful. In these cases, it is interesting that the dependence of the bending energy on the overall film topology vanishes when one chooses  $\lambda = \bar{\lambda}$  and the effective Gaussian curvature modulus is then zero. This can simplify many calculations of the energetics and fluctuations of complex surfaces.

### 3.4. Curvature energy

One can also discuss the curvature energy using symmetry considerations and relate it to the models analysed previously. The most general form of the curvature free energy  $f_c$ , *per unit area*, up to quadratic order in the two curvatures, can be written in terms of the mean and Gaussian curvatures defined previously. One can write

$$f_c = \frac{1}{2}k(H - c_0)^2 + \bar{k}K. \quad (3.13)$$

This form for the free energy per unit area was discussed by Helfrich [8] and states that the mean curvature which minimizes the free energy has a value  $c_0$ , termed the *spontaneous curvature* of the membrane. The energy cost of deviating from the spontaneous curvature is the *bending or curvature modulus*  $k$ . The parameter  $k$ , known as the *saddle-splay modulus*, measures the energy cost of saddle-like deformations.

The spontaneous curvature describes the tendency of the surfactant film to bend towards either the water ( $c'_0 < 0$  by convention) or the oil ( $c'_0 > 0$ ). For amphiphilic membranes, it is taken (in the absence of long-range interactions) to arise from the competition between the packing areas of the polar head and hydrocarbon tail of the surfactant molecules. If the interactions between the polar heads (as mediated through the intervening water and electrolyte) favour a smaller packing area than that dictated by the tail–oil–tail interactions, the surfactant film will tend to curve so that the heads (and the water) are on the ‘inside’ of the interface. The bending moduli  $k$  and  $\bar{k}$  arise from the elastic constants determined by the head–head and tail–tail interactions. In section 5 we show how these moduli depend on the surfactant chain length and on the head–head interaction strength.

The bending parameters  $c_0$ ,  $k$  and  $\bar{k}$  can be derived from equations (3.6) and (3.7). Comparing equations (3.6), (3.7) and (3.13) and noting that  $f$  is an energy per molecule, while  $f_c$  is an energy per unit area, we identify

$$k = \frac{2g_2}{\Sigma_0}, \quad (3.14)$$

$$\bar{k} = \frac{\bar{g}_2}{\Sigma_0}, \quad (3.15)$$

$$c_0 = -\frac{g_1}{2g_2}. \quad (3.16)$$

This allows the curvature moduli to be obtained from the parameters of a given microscopic model that incorporates both the change in the area per molecule and the curvature. We note that a stable film will always have  $k > 0$ . However, the sign of  $\bar{k}$  can be either positive or negative; films that prefer isotropic shapes (where the Gaussian curvature  $K > 0$ ) such as spheres or planes will have  $\bar{k} < 0$ , while films that prefer saddle shapes (where the Gaussian curvature  $K < 0$ ) will have  $\bar{k} > 0$ . One can show that the requirement that the quadratic term be positive definite implies that films are only stable if (for values of  $\bar{k} < 0$ )  $2k + \bar{k} > 0$ ; otherwise higher-order curvature terms are needed to stabilize the system.

### 3.5. Thermodynamics of self-assembling fluid interfaces

#### 3.5.1. Self-assembly in solution

The previous section presented a mechanical picture of the perturbations of the molecules in a thin film whose degrees of freedom were the area per molecule and the film curvature. In this section, we show that, even if one considers an additional degree of freedom, namely the ability of molecules in the film to resolubilize in the solvent, one still can use a bending energy description of the film energetics, provided that one is not too close to the critical concentration at which the films first self-assemble from solution. For simplicity, and because most cases of self-assembling films occur for fluid films, we discuss this case here. The bending energy of a solid film is treated later.

We consider a fluid monolayer membrane at a water–oil interface in equilibrium with dilute solutions of the very same amphiphiles in the water and oil. In general, there is an equilibrium between the amphiphiles adsorbed at the interface and those in the bulk solution. For extremely small volume fractions of amphiphile, the surfactants will preferentially remain in solution owing to their higher entropy of mixing with the solvent; the interface will have a relatively small number of amphiphiles adsorbed per unit area. However, this is not the case when the amphiphilic molecules are strongly insoluble in either solvent owing to the unfavourable interactions of the polar groups with hydrocarbon solvents and of the hydrocarbon groups with polar solvents. The large energy cost of keeping these molecules in solution overcomes their entropy of mixing and at even moderately small volume fractions (which in practice can be very low, about  $10^{-4}$  or less for surfactants which strongly prefer the interface), the free-energy cost for remaining in solution is too high and the amphiphiles will tend to accumulate at the interface.

As one increases the volume fraction of amphiphiles in the solution, more and more would go to the interface and the area  $\Sigma$  per molecule on the interface would decrease. However, the molecules cannot pack at infinite density at the interface. In the case where there exists a minimum in the packing energy of the flat interface at a value of  $\Sigma = \Sigma_0$ , the system will keep adding amphiphiles to the flat interface until  $\Sigma$  is reduced to a value close to  $\Sigma_0$ . If even more molecules are added to the system, instead of decreasing  $\Sigma$  further and thus *increasing* the free energy (since  $\Sigma = \Sigma_0$  is a minimum), the amphiphiles will maintain their packing at  $\Sigma \approx \Sigma_0$  and accommodate the extra molecules by creating *more* interface (e.g. by rippling the flat interface or by incorporating oil into the water with the additional molecules located at the extra interface that is thus generated). When this happens, one says that the interface is saturated; instead of changing the packing area, the system accommodates more amphiphiles by making more interface while still minimizing the packing free energy with respect to  $\Sigma$ . Of course, the interface may then have some curvature and the actual value of  $\Sigma$  may depend on the curvature.

In general, one must consider the chemical potential of a molecule at the interface and in the solution. The equality of these two chemical potentials is the criterion for equilibrium and hence determines the area per molecule on the interface. When the amount of interface is fixed, as in the case of a single water–oil interface, this equality fixes  $\Sigma$ . However, when the amount of interface can vary to minimize the free energy,  $\Sigma$  is determined by minimizing the interfacial free energy per molecule; the chemical potential then determines the *number* of interfaces that exist in the system as well as the (small) volume fraction of surfactant that is not incorporated in these interfaces; the properties of *each* interface are determined to a first approximation by the minimization of the local free energy of the film.

The thermodynamics of these processes are discussed in detail in the following section and in [10], where it is shown that there is a critical volume fraction  $\phi_s^c$  of surfactant above which there are many interfaces in the system, and the amount of surfactant not incorporated into these interfaces is small and remains approximately constant as the overall amount  $\phi_s$  of surfactant is increased ( $\phi_s^c$  is analogous to a critical micelle concentration [1]) [2]. One usually considers the simple case of surfactants that are strongly surface active (highly insoluble in the bulk) so that at even very small volume fractions of amphiphile ( $\phi_s^c \ll \phi_s \ll 1$ ), there are *many* interfaces (e.g. vesicles and microemulsions) in the system in equilibrium. In this approximation, the fraction of surfactants in solution is very small and their volume

fraction is approximately constant. However, in the following section we show how the equilibrium between the surfactant in the film and in the solution can be taken into account; the net effect is to soften the bending constants (i.e., the renormalized moduli are functions of  $\phi_s$ ); this is a major effect for the case where  $\phi_s \approx \phi_s^c$ .

Once the appropriate bending free energy has been derived, the properties of the system are obtained by focusing on the physics of the interfaces. When, in addition, the fluctuations of and interactions between these interfaces and their translational entropy can be neglected compared with the local deformation energies of the films (true when  $k \gg k_B T$ ) one can first minimize these local deformation energies to find the size and shape of the interfaces. Afterwards, one can finally take into account the entropic and interaction effects as higher-order corrections to the shape which is primarily determined by the curvature energy.

In addition to being characterized by the area per amphiphile, the interfacial membrane is also characterized by its thickness  $\lambda$ , which can also change under deformations of the film. For simplicity, we assume that the equation of state of the flat membrane determines the thickness as a function of the area per molecule. (A simple example is the case of an incompressible film where the product of  $\lambda \Sigma$  is constrained to equal the molecular volume so that  $\lambda \sim 1/\Sigma$ .) We thus take the flat membrane to be characterized only by the area  $\Sigma$  per molecule; the curved membrane is characterized by both its curvature and the area per molecule.

### 3.5.2. Free energy of self-assembling interfaces

First consider a single, locally flat isolated interface. Saturation occurs when the interfacial free energy achieves a minimum:

$$\frac{\partial f_0}{\partial \Sigma} = 0, \quad (3.17)$$

where  $f_0$  is the free energy per molecule for a flat layer and  $\Sigma$  is the area per molecule. The free energy per molecule is minimized when  $\Sigma = \Sigma_0$ . The optimal value of the area per molecule arises from a balance of terms such as the entropy, and the interfacial tension terms or attractions. The entropy favours a large area per molecule (because of the larger number of centre-of-mass positions and chain conformations) while the interfacial tension terms (e.g. contact of the hydrocarbon chains with the water) and molecular (e.g. van der Waals) attractions favour a small value of  $\Sigma$ . Of course, there can be deviations in the area per molecule from this minimum and the energy cost of such a compression or expansion is

$$\Delta f_0 = \frac{1}{2} f_0'' (\Sigma - \Sigma_0)^2, \quad (3.18)$$

where the primes signify a derivative with respect to  $\Sigma$ . However, these deformations are typically of higher energy than the curvature deformations; a membrane can change its shape or size with a much lower free-energy cost than that required to compress or expand it. Below, we show how these fluctuations soften the bending moduli of the system; however, the basic picture of a set of films with curvature elasticity is maintained even if one allows area fluctuations. It is important to remember therefore that, for insoluble amphiphiles, it is the saturation of the interface and the minimization of the area per molecule that permits the usual surface tension term to be neglected; the derivative  $\partial f / \partial \Sigma = 0$ . The surface tension is no longer relevant since the molecules adjust their area to optimize the free energy



and it is therefore the curvature energy that mainly determines the properties of the film.

The standard treatment of curvature elasticity focuses on the compressibility and bending elasticity of isolated interfaces. The free energy of an interfacial film with fixed curvature and a fixed number of surfactants is minimized with respect to the area per molecule, and the bending energy is then derived. In reality, the number of molecules which comprise these interfaces is not fixed since they coexist and exchange with the surfactant monomers in the solution. In what follows we show that, even in this case, one can still derive an effective bending free energy for the surfactant film. The curvature energy is obtained by minimization of the total free energy of both the surfactant molecules in the film as well as the molecules in the solution with which they exchange. The effect of monomers in the solution has also been discussed in the context of block copolymer self-assembly [10]. Here we use a similar formalism to calculate the effective curvature energy and to examine its dependence on the surfactant volume fraction. It is found that the presence of surfactant molecules in the solution induces softening of the film, that is, the effective curvature moduli decrease from their nominal values. Additionally, we show how the adjustment of the area per surfactant upon bending can further soften the elastic parameters of the film.

To be specific, we consider a system of surfactant monolayers in a water–oil–surfactant microemulsions (the same conclusions also apply to bilayers in a one-component solution). The volume fractions of water and oil, which are assumed to be mutually insoluble, are  $\phi_w$  and  $\phi_o$ , respectively and the total volume fraction of amphiphile in the system is  $\phi_s$ . The surfactant molecules are partitioned among the water, the oil, and the monolayer films with volume fractions  $\phi_s^w$ ,  $\phi_s^o$  and  $\phi_s^f$  respectively. The local concentrations of surfactant in water and oil are  $\psi_w$  and  $\psi_o$  respectively (it is assumed that the water and oil do not penetrate the film so that the local concentration of surfactant in the film is  $\psi_s = 1$ ). The local surfactant volume fractions  $\psi_o$  and  $\psi_w$  are related to the concentrations  $\phi_s^o$  and  $\phi_s^w$  relative to the whole system by

$$\begin{aligned}\psi_o &= \frac{\phi_s^o}{\phi_o + \phi_s^o}, \\ \psi_w &= \frac{\phi_s^w}{\phi_w + \phi_s^w},\end{aligned}\tag{3.19}$$

Since we focus on the case where the surfactant is highly insoluble in the water and oil regions, we assume that the amphiphile in these regions can be described as an ideal gas of molecules. However, the main conclusions remain valid even for interacting monomers in the solution. The free energies  $f_w$  and  $f_o$ , per unit volume of the surfactant molecules in the water and oil regions respectively can be written as

$$\begin{aligned}f_w &= \psi_w (\log \psi_w - 1 + \chi_w), \\ f_o &= \psi_o (\log \psi_o - 1 + \chi_o),\end{aligned}\tag{3.20}$$

where  $\chi_w$  and  $\chi_o$  are the energies (in units of  $k_B T$ ) of one molecule solubilized in water and oil respectively relative to the same molecule in a flat lamellar configuration (taken to be the zero of energy). In equation (3.20),  $f_w$  and  $f_o$  are taken in units of  $k_B T / v_0$ , where  $v_0$  is the volume per molecule and  $T$  is the temperature.

The surfactant film is characterized by a free energy  $f_i(\Sigma, H, K)$  per molecule, which depends on the area  $\Sigma$  per molecule, the mean curvature  $H$  and the Gaussian curvature  $K$ . In what follows we shall use an expansion to quadratic order in the curvature:

$$f_i(\Sigma, H, K) = f_0(\Sigma) + f_1(\Sigma)H + f_2(\Sigma)H^2 + \bar{f}_2(\Sigma)K \quad (3.21)$$

appropriate for small curvature [2]. This free energy also includes the contributions from the short-range interactions of the film with the water and oil molecules. The total free energy  $f_T$  per unit volume includes the energy  $(\phi_w + \phi_s^w)f_w$  of the surfactant in the water region and the energy  $(\phi_o + \phi_s^o)f_o$  of the molecules in the oil region. (Note that the water phase is composed of water and the dissolved surfactant, and occupies a fraction  $\phi_w + \phi_s^w$  of the total volume. A similar expression applies for the oil phase.) The contribution of the film energy to the total energy is  $\phi_s^f f_i$ . Thus, the total energy is

$$f_T = (\phi_o + \phi_s^o)f_o + (\phi_w + \phi_s^w)f_w + \phi_s^f f_i. \quad (3.22)$$

We are interested in the limit of low solubility of the surfactant molecules in both water and oil, when  $\phi_s^{o,w} \ll \phi_{o,w}$ , and the total energy  $f_T$  per unit volume is thus approximated by  $f_T = \phi_o f_o + \phi_w f_w + \phi_s^f f_i$ . This form of free energy assumes extensivity of the system, that is the energies are calculated for isolated films and the entropy of mixing, and the interactions among the films are neglected. This assumption is valid since the entropy (per unit volume) of the self-assembled films is smaller by a factor of  $R^{-3}$  than the entropy of the same amount of separate surfactant molecules, where  $R$  is a characteristic size of a microemulsion droplet. The interaction energy can be neglected as long as the solution is dilute. Here we neglect both the entropy and the interactions in the calculation of the local packing area and the curvature energy and keep the curvatures and size of the microemulsion regions fixed. Of course, to determine these latter properties of the films, one *must* include entropy and interactions in the minimization of the free energy with respect to  $H$  and  $K$ .

### 3.5.3. Free-energy minimization; effective modulus

In what follows the total free energy  $f_T$  is minimized with respect to all the other degrees of freedom: the surfactant concentrations  $\psi_o$ ,  $\psi_w$  and  $\phi_s^f$  in each region, and the area  $\Sigma$  per molecule in the film. The system is defined by its composition  $\phi_w$ ,  $\phi_o$  and  $\phi_s$  and by the fixed curvatures  $H$  and  $K$ . This procedure enables us to derive an effective curvature energy which does take into account the effect of the monomers in the solution. The free energy  $f_T$  is minimized subject to the constraint of conservation of the total amount of the surfactant:

$$\phi_s^w + \phi_s^o + \phi_s^f = \phi_s. \quad (3.23)$$

For low solubility of the surfactant it follows from equation (3.19) that the constraint of equation (3.23) can be approximated by  $\phi_w \psi_w + \phi_o \psi_o + \phi_s^f = \phi_s$ . The constrained minimization with respect to  $\psi_o$ ,  $\psi_w$  and  $\phi_s^f$  is calculated using the method of Lagrange multipliers. The physical equivalent of this procedure is that all three regions contain surfactants with the same chemical potential which turns out to be proportional to  $f_i(\Sigma, H, K)$ , the energy per surfactant in the film. One finds that the values at the minimum are

$$\begin{aligned}\psi_o &= \exp(f_i - \chi_o), \quad \psi_w = \exp(f_i - \chi_w), \\ \phi_s^f &= \phi_s - \phi_o \psi_o - \phi_w \psi_w.\end{aligned}\tag{3.24}$$

The physical situation is completely analogous to micellization. There is a critical volume fraction  $\phi_s^c$  of surfactant, below which all the surfactant monomers are in the solution [10]. It is determined from equation (3.24) with  $\phi_s^f = 0$  to be

$$\phi_s^c = \phi_o \psi_o + \phi_w \psi_w.\tag{3.25}$$

Only for larger values of volume fraction,  $\phi_s > \phi_s^c$ , do the film layers begin to appear. With the ratio  $\phi_w/\phi_o$  of water to oil kept constant, one can relate the volume fractions by

$$\phi_s^f = \frac{\phi_s - \phi_s^c}{1 - \phi_s^c}.\tag{3.26}$$

The total energy per unit volume obtained after minimization is

$$f_T = \phi_w(f_i - 1) \exp(f_i - \chi_w) + \phi_o(f_i - 1) \exp(f_i - \chi_o) + \phi_s^f f_i.\tag{3.27}$$

One can define an effective curvature energy per surfactant molecule of  $f^* \equiv f_T/\phi_s$  ( $f^*$  is in units of  $k_B T$ ). In previous treatments, the surfactant was treated as totally insoluble,  $\psi_o = \psi_w = 0$ , and the effective energy is equal to the bare curvature energy,  $f^* = f_i$ ; here we determine the correction to  $f_i$  from the finite solubility of the surfactant. In the remaining discussion it is assumed, as a matter of convenience<sup>†</sup>, that the solubilities in the water and the oil are equal:  $\chi_w = \chi_o = \chi$ . The effective free energy now takes a simplified form:

$$f^* = f_i - \frac{1 - \phi_s}{\phi_s} \exp(f_i - \chi).\tag{3.28}$$

Of course, the system also responds to changes in the curvature by adjusting the area per molecule to minimize the total energy. We find that this tends to reduce further the bare bending modulus  $f_2$  by an amount related to the spontaneous curvature. Expansion of the generic form of the film energy to second order in the change of the area  $\Sigma$  per molecule (equation (3.21)) yields<sup>‡</sup>

<sup>†</sup> In the case where  $\chi_w \neq \chi_o$  the physical conclusions concerning the influence of the monomers do not change, but the expressions are slightly more complicated.

<sup>‡</sup> For cases where the curvatures are small compared with the inverse of the film thickness, it is possible to choose the plane from which the curvature is measured so that the term linear in both the curvature  $H$  and the change  $\Sigma - \Sigma_0$  in the area compared with the flat layer has a coefficient which is zero [2]. This choice for the dividing surface is termed the *neutral surface* and allows the area and curvature degrees of freedom to be decoupled. On the neutral surface, the free energy is minimal when the area per molecule is always equal to the area per molecule in the flat geometry and the free energy includes only the curvature terms. In what follows, however, we consider a general surface where the coupling of the area and curvature terms is non-zero. We show that this still yields the Helfrich curvature free energy, but with a renormalized bending coefficient. The reason for not necessarily choosing a neutral surface is that microscopic treatments of curved thin films often are conveniently formulated in terms of a physical dividing surface, such as the polar head group in a system of simple surfactants or the connecting point in a block copolymer, which does not necessarily coincide with the neutral surface.

$$f_t(\Sigma, H, K) = f_0(\Sigma_0) + \frac{1}{2}f''(\Sigma_0)(\Sigma - \Sigma_0)^2 + f_1(\Sigma_0)H + f_1'(\Sigma_0)(\Sigma - \Sigma_0)H + f_2(\Sigma_0)H^2 + \bar{f}_2(\Sigma_0)K, \quad (3.29)$$

where  $\Sigma_0$  is the area per molecule at the minimum of the flat film free energy  $f_0$ . Substitution of equation (3.29) into equation (3.28) and minimizing with respect to  $\Sigma$  yields  $\partial f_t / \partial \Sigma = 0$ , that is the area per molecule at the minimum of the effective energy  $f^*$  has the same value of the area per molecule at the minimum of  $f_t$ :

$$\Sigma^* = \Sigma_0 - \frac{f_1'}{f_0''} H. \quad (3.30)$$

Substitution of  $\Sigma^*$  back into equation (3.28) and expansion of the curvature part of the free energy,  $f_t - f_0 \ll f_t$ , yields

$$f^* = f_0^* + f_1^* H + f_2^* H^2 + \bar{f}_2^* K, \quad (3.31)$$

with the coefficients

$$\begin{aligned} f_0^* &= f_0 + r - 1, \\ f_1^* &= f_1 r, \\ f_2^* &= \left( f_2 - \frac{1}{2} \frac{f_1'^2}{f_0''} \right) r \end{aligned} \quad (3.32)$$

and  $\bar{f}_2^* = \bar{f}_2 r$ , where

$$r = 1 - \frac{1 - \phi_s}{\phi_s} \exp(f_0 - \chi). \quad (3.33)$$

The area fluctuations thus serve to reduce the bare bending modulus  $f_2$  by an amount proportional to the square of the spontaneous curvature  $f_1'$  divided by the compressibility; for very incompressible systems (large values of  $f_0''$ ), these changes are small while, for anomalously compressible systems, this softening effect can be more significant. In any case, the expression for the change in  $f_2$  is always negative; the extra degree of freedom of the area allows the system to lower its free energy.

We now return to the effect of the fluctuations in the surfactant between the film and the solution. Comparison of the coefficients of  $f^*$  with equations (3.29)–(3.33) shows that  $r$  is also the ratio  $r = k^*/k = \bar{k}^*/\bar{k}$  of the effective to the nominal curvature moduli. The spontaneous curvature remains the same:  $c_0^* = c_0$ . Using the definition of  $\phi_s^c$ , equation (3.33) can be rewritten in the form

$$r = \frac{1 - \tilde{\phi}_s^c / \phi_s}{1 - \tilde{\phi}_s^c}, \quad (3.34)$$

where  $\tilde{\phi}_s^c = \phi_s^c(H = K = 0)$  is the critical volume fraction for creation of flat interfaces (we note that  $\phi_s^c$  depends upon the curvature energy). In figure 4 we show a plot of  $r$  against  $\tilde{\phi}_s^c / \phi_s$ . It is evident that even for high surfactant concentrations there is a correction that behaves like  $k - k^* = k \tilde{\phi}_s^c / \phi_s$ . As  $\phi_s$  decreases, the effective curvature moduli decrease until they vanish at the critical volume fraction  $\tilde{\phi}_s^c$ :

$$k(\phi_s = \tilde{\phi}_s^c) = \bar{k}(\phi_s = \tilde{\phi}_s^c) = 0. \quad (3.35)$$

The mechanism underlying the softening of the curvature moduli arises from the ability of the surfactant molecules inside the film to exchange with monomers in the

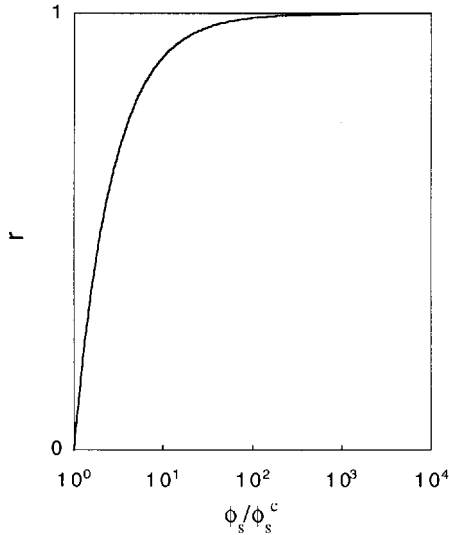


Figure 4. Renormalization factor  $r$  which quantifies the softening of the bending moduli as a function of the ratio of the surfactant volume fraction  $\phi_s$  to its critical value  $\phi_s^c$ , where the film layers first occur. The factor  $r$  is approximately given by  $r \sim 1 - \tilde{\phi}_s^c / \phi_s$ , where  $\tilde{\phi}_s^c$  is the critical surfactant volume fraction for the occurrence of flat sheets, as discussed in the text.

solution. If the system composition is near critical,  $\phi_s \approx \phi_s^c$ , there is a small amount of surfactant in the films,  $\phi_s^f \ll \phi_s^c$ . Now, if one slightly increases the curvature energy  $f_i$  of the film, the solubilities  $\psi_w = \exp(f_i - \chi_w)$  and  $\psi_o = \exp(f_i - \chi_o)$  will increase and surfactant molecules from the films will be transferred to the solution. Hence, the average free energy  $f^*$  per molecule, will not increase according to the nominal curvature moduli but according to their decreased value, which takes into account the free energy of the molecules in the solution. This is a major effect for relatively small surfactant volume fractions, when there is a small amount of amphiphile in the films. In this case, when the curvature energy is increased, relatively large portions of the films can be reabsorbed in the solution. However, when there are many interfaces in the system, only a negligible fraction of the surfactant can be reabsorbed in the solution, and thus the corrections to the nominal values of curvature moduli are small. In this case, where  $\phi_s \gg \tilde{\phi}_s^c$ , the microemulsion can be approximated by a system in which the surfactant molecules are totally insoluble and are (nearly) all contained at the interfaces. This is the situation usually treated and discussed in the remainder of this review, where one considers only the film energy and then optimizes the packing area at fixed curvature in order to derive the curvature free energy.

In summary, we have shown that, when the exchange of the molecules in the film with those in the solution is taken into account, the curvature moduli are decreased. The nominal moduli are renormalized by a factor which depends on the volume fraction of the surfactant. The curvature moduli vanish at the critical concentration. For amphiphile volume fractions much larger than the critical value, the correction is small and the films are thus well approximated by a system in which all the surfactant is the film. The softening phenomenon, which also occurs for compressible

films as the area per molecule adjusts to the curvature, resulting in a reduction in the bending moduli, is an example of a general physical principle, which suggests that the free energy of a system decreases when one removes constraints. Here the constraint which was removed is the requirement of either fixed area or that all the surfactant is contained in the films.

### 3.6. Pressure and bending

#### 3.6.1. Work of deformation

For small curvatures, equation (1.1) shows that the curvature energy of a thin film is characterized by the three parameters  $k$ ,  $\bar{k}$  and  $c_0$ . The qualitative behaviour of any system, including such properties as the equilibrium shapes, magnitude of thermal fluctuations and any phase transitions, can of course be calculated as a function of these constants. However, the physics of the system can be radically different depending on the physical parameters; for example a change in  $c_0$  can induce shape changes in the system. It is thus of interest to relate the bending elastic moduli and the spontaneous curvature to the physics of the particular system. This section first shows how these parameters are related to the pressure distribution in the membrane which is a general property of thin fluid films. Applications of these ideas occur in calculations of the bending elastic constants of charged membranes where the pressure distribution arises from the spatially dependent counterion concentration [11–14] and in the bending of block copolymer films where the pressure distribution is related to the monomer density [10, 15–17]. Both these cases are briefly reviewed in the subsequent discussion of microscopic models. The case of a solid thin film is also treated below. A treatment for the bending energy of liquid interfaces which deals with concentration gradients at liquid–liquid boundaries with no explicit reference to the surfactant properties (which are the focus of the present discussion), can be found in [18].

The bending elastic moduli are determined by the curvature dependence of the free energy of the system, that is, there is a resistance of the system to curvature. This curvature dependence is associated with a local area change; curvature changes the local area element. For an isotropic and homogeneous fluid, the work done in changing the volume is calculated using the relationship

$$\Delta F = - \int_{V_0}^V \Pi(V') dV', \quad (3.36)$$

where  $\Delta F$  is the change in free energy due to an incremental volume change from  $V_0$  to  $V$  and  $\Pi(V)$  is the local pressure (for a compressible system) or osmotic pressure (for a system of solvent and solute) against which this work is done. In general,  $\Pi$  can be a function of  $V$  and equation (3.36) accounts for the total work that is done in expanding the system from  $V_0$  to  $V$ ; this requires a knowledge of  $\Pi$  at all volumes between  $V$  and  $V_0$  and not just  $\Pi(V_0)$ . However, thin liquid films that show a resistance to bending are anisotropic and one must consider separately the longitudinal pressure  $\Pi_\ell$ , which resists changes in the film thickness and the transverse pressure  $\Pi_t$  which resists changes in the film area. In general, these quantities may vary within the film.

For solid films (i.e., films with a shear modulus), there is an additional resistance to bending arising from the resistance to shear deformations [19]. This results in a non-zero curvature modulus even for a system which is elastically isotropic in the

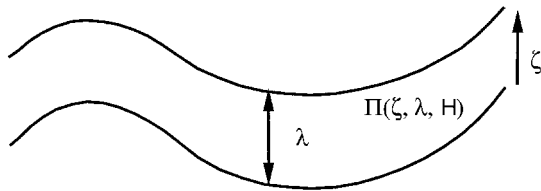


Figure 5. Thin film of overall thickness  $\lambda$ ; the pressure varies along the thickness  $\zeta$ .

bulk as is discussed below. This is not the case for systems with zero shear modulus treated in this section; completely isotropic fluids show no resistance to bending deformations.

The curvature energy is essentially the work done in changing the *local* volume of the membrane related to the change in the area element due to the curvature; this work is done even if there is no *global* change in the volume of the membrane. We shall therefore use a local version of equation (3.36) to calculate the curvature energy and consider the volume change due to curvature. This method for calculating the bending energy was introduced in [16, 20] where the area change was considered.

We consider an infinitely large membrane of thickness  $\lambda$  and area  $\Sigma$  per molecule (defined on the ‘lower’ ( $\zeta = 0$ ) plane of the membrane (figure 5) and calculate the curvature free energy as a function of these parameters that characterize the global properties of the membrane. In practice, both  $\Sigma$  and  $\lambda$  are functions of curvature. However, it is simplest first to keep these parameters fixed and to derive the curvature energy expansion; this requires that we know  $\Pi$  for any given  $\Sigma$  and  $\lambda$ . Afterwards, one can minimize the free energy with respect to these parameters (equivalent to determining an equation of state) and/or use constraints of constant volume to constrain either or both of them. (See section 3.2 for an example of how the equilibration of the area per molecule can affect the bending modulus.) For example, the thickness of the membrane can be found by requiring that the curvature energy includes only pure curvature deformations, that is that there is no overall compression or expansion of the membrane. Here, we make this choice and determine the film thickness  $\lambda$  of the curved film by requiring that the total volume of the system is kept constant (enforcing global incompressibility).

For constant or slowly varying curvatures, the area element changes owing to the curvature. The equality of the volumes of the flat and curved membranes is written (see equation (2.20) and the discussion in section 2 on parallel surfaces):

$$\Sigma \int_0^\lambda d\zeta (1 + 2\zeta H + \zeta^2 K) = \Sigma_f \lambda_f, \quad (3.37)$$

where  $\lambda_f$  is the thickness and  $\Sigma_f$  is the area per molecule of the flat membrane. The coordinate  $\zeta$  is the distance from the lower surface of the membrane in the normal direction, and  $H$  and  $K$  are the mean and Gaussian curvatures respectively. To take into account the effects of the change in the area per molecule we define

$$\lambda_0 = \lambda_f \frac{\Sigma_f}{\Sigma}. \quad (3.38)$$

We therefore include all the dependence of the parameters on the actual area  $\Sigma$ , per molecule of the curved membrane in their behaviour as a function of  $\lambda_0$  and rewrite equation (3.37) as

$$\int_0^\lambda d\zeta (1 + 2\zeta H + \zeta^2 K) = \lambda_0. \quad (3.39)$$

As mentioned previously, once the curvature energy expansion is obtained in terms of  $\lambda_0$ , it can further be minimized over  $\Sigma$  and the ‘area-equilibrated’ expansion can be derived as was done in section 3.2. This implies that, under the constraint of constant local volume, the thickness  $\lambda$  of the curved membrane is related to the thickness  $\lambda_0$  of the flat membrane by

$$\lambda \left( 1 + \lambda H + \frac{K\lambda^2}{3} \right) = \lambda_0. \quad (3.40)$$

To second order in the curvatures, this implies that

$$\lambda \approx \lambda_0 \left( 1 - \lambda_0 H - \frac{K\lambda_0^2}{3} + 2\lambda_0^2 H^2 \right). \quad (3.41)$$

### 3.6.2. Bending moduli

We assume that the curvatures are slowly varying in the plane of the membrane (or are constant as they are for cylindrical and spherical curvature) so that the pressure depends only on  $\zeta$ . The surface of curvature is measured from the lower plane of the membrane located at  $\zeta = 0$ . We calculate  $f_c$ , which is the additional curvature free energy per unit area (the (flat) base area is  $A_0$ , which we hold fixed for now) from the change  $A_0(2\zeta H' + \zeta^2 K')$  in the local area due to the imposition of the curvatures  $H'$  and  $K'$ . Using the principle of virtual work to compute the free energy, we note that the work is independent of the path chosen. Thus, we choose first to keep the thickness fixed at  $\lambda_0$  and to change the area elements commensurate with the curvature. Since we shall need contributions up to second order in the curvature, we consider the work done in continuously changing the mean curvature from  $H' = 0$  to  $H' = H$  and the Gaussian curvature from  $K' = 0$  to  $K' = K$ ; the mean and Gaussian curvatures are two independent degrees of freedom of the membrane as discussed in section 2. This requires an integration over the differential changes in curvature. We then have a curved membrane of thickness  $\lambda_0$ . For this process of local area change, it is the *transverse pressure*  $\Pi_t$  that does work against the differential volume change; the initial volume element  $A_0(1 + 2H'\zeta + K'\zeta^2) d\zeta$  is modified because of the change in the area element upon increasing  $H'$  by  $dH'$  and  $K'$  by  $dK'$ :

$$dV = A_0(2\zeta dH' d\zeta + \zeta^2 d\zeta dK'). \quad (3.42)$$

Next, we compute the work needed to change the thickness of this curved membrane from  $\lambda_0$  to  $\lambda$ . Here, the membrane surface at  $\zeta = \lambda'$  does work against the change in the thickness and we compute this work by multiplying the *longitudinal pressure*  $\Pi_\ell$  at the top surface by the volume element  $d\lambda'$  and integrating  $\lambda'$  from  $\lambda_0$  to  $\lambda$ . We therefore write

$$f_c = -f_a - f_t, \quad (3.43)$$

where



$$f_a = f_H + f_K \quad (3.44)$$

$$f_H = \int_0^H dH' \int_0^{\lambda_0} d\zeta 2\zeta \Pi_t(\zeta, \lambda_0, H', K') \quad (3.45 a)$$

$$f_K = \int_0^K dK' \int_0^{\lambda_0} d\zeta \zeta^2 \Pi_t(\zeta, \lambda_0, H', K'), \quad (3.45 b)$$

$$f_t = \int_{\lambda_0}^{\lambda} d\lambda' \Pi_\ell(\lambda', \lambda', H, K) (1 + 2H\lambda' + K\lambda'^2), \quad (3.46)$$

where  $\Pi_t(\zeta, \lambda_0, H', K')$  is the local  $\zeta$ -dependent transverse pressure in the membrane of thickness  $\lambda$ , which is bent with the mean curvature  $H'$  and the Gaussian curvature  $K'$ . The longitudinal pressure  $\Pi_\ell$  is also a function of the thickness and the curvature. The term  $f_a$  is the work due to the change in the area element at fixed  $\lambda = \lambda_0$  and the term  $f_t$  is the work due to the change in thickness of the already bent membrane. This form for  $f_c$  guarantees that the curvature energy is calculated relative to the flat state; that is, if  $H = K = 0$  (and thus  $\lambda = \lambda_0$ ), the bending energy must vanish. More importantly, equations (3.43)–(3.46) have the property that any constant isotropic terms in the pressures do *not* contribute to the curvature energy  $f_c$ . This can be seen explicitly using equation (3.40) for  $\lambda$  in equations (3.43)–(3.46) with  $\Pi_t = \Pi_\ell$  equal to a constant. The physical reason for this is that the curvature energy requires an interaction that extends throughout the thickness of the membrane; an ideal gas or small molecule fluid with constant density and hence constant  $\Pi_t = \Pi_\ell$  takes the shape of its container and in the absence of compression or expansion, guaranteed by equation (3.40), has zero curvature energy.

In principle, to evaluate the curvature energy we must know the pressures at all values of the intermediate curvatures  $H'$  and  $K'$ . However, to find  $f_c$  to second order in the curvature, it is sufficient to expand each of the pressures  $\Pi_i$  ( $i = t, \ell$ ), to first order in  $H$  and we write:

$$\Pi_i(\zeta, \lambda, H', K') \approx \Pi_{i0}(\zeta, \lambda) + \left( \frac{\partial \Pi_i}{\partial H'} \right)_{H=0} H' + \dots, \quad (3.47)$$

where  $\Pi_{i0}(\zeta, \lambda)$  is the local transverse ( $i = t$ ) or longitudinal ( $i = \ell$ ) pressure of a membrane with thickness  $\lambda$  in the flat state. Equation (3.47) requires that we solve for the free energy of the membrane in the curved state; that is we must solve the entire problem to linear order in curvature, obtain the pressure and then take the curvature derivative. We use this expansion in both  $f_a$  and  $f_c$  and perform the integrals over the dummy curvature variables in  $f_a$ . The contribution from  $f_t$  is evaluated by expanding the integral for small values of  $\lambda - \lambda_0$  (see equation (3.41)) to second order. Keeping terms up to second order in curvature, we find that

$$\begin{aligned} f_c = & - \int_0^{\lambda_0} d\zeta \left[ \Pi_{t0}(\zeta, \lambda_0) (2\zeta H + \zeta^2 K) + \left( \frac{\partial \Pi_t}{\partial H} \right)_{H=0} H^2 \zeta \right] \\ & - \lambda_0 \left( -\lambda_0 H - \frac{K\lambda_0^2}{3} \right) \Pi_{t0}(\lambda_0, \lambda_0) + \lambda_0^2 H^2 \left( \frac{\partial \Pi_\ell(\lambda_0, \lambda_0)}{\partial H} \right)_{H=0} \\ & - \frac{1}{2} \lambda_0^4 H^2 \left( \frac{\partial \Pi_\ell(\lambda', \lambda')}{\partial \lambda'} \right)_{\lambda'=\lambda_0}. \end{aligned} \quad (3.48)$$

Comparing powers of  $H$ ,  $H^2$  and  $K$  in equations (3.13), (3.40) and (3.48) allows us to identify the curvature moduli as moments of the pressure distribution.

We now present the results for the curvature moduli in terms of the pressure distribution through the thin film. We define the longitudinal and transverse pressures in the flat film as  $\Pi_{\ell 0}(\zeta, \lambda_0)$  and  $\Pi_{t 0}(\zeta, \lambda_0)$ ; the subscript 0 on  $\Pi$  and  $\lambda$  indicates that these are the values for the flat film. The work done to bend the film can be calculated in terms of the pressure distribution in the film [2] and the result is the curvature elastic energy of equation (1.1). The elastic constants are given by

$$k_{c0} = 2 \int_0^{\lambda_0} \tilde{\Pi}_0(\zeta, \lambda_0) \zeta d\zeta \quad (3.49)$$

$$\bar{k} = - \int_0^{\lambda_0} \tilde{\Pi}_0(\zeta, \lambda_0) \zeta^2 d\zeta \quad (3.50)$$

$$k = -2 \int_0^{\lambda_0} \left\{ \left[ \frac{\partial \tilde{\Pi}_0}{\partial H} \right]_{H=0} - \left( \left[ \frac{\partial \Pi_{\ell}(\lambda_0, \lambda_0)}{\partial H} \right]_0 + \left[ \frac{\partial \Pi_{\ell}(\lambda, \lambda)}{\partial (1/\lambda)} \right]_{\lambda=\lambda_0} \right) \right\} \zeta d\zeta \quad (3.51)$$

where

$$\tilde{\Pi}_0(\zeta, \lambda_0) = \Pi_{t 0}(\zeta, \lambda_0) - \Pi_{\ell 0}(\lambda_0, \lambda_0). \quad (3.52)$$

If the pressure field is continuous in space, then the thickness,  $\lambda_0$  can be set to infinity and  $\Pi_{\ell 0}(\lambda_0, \lambda_0) = 0$ , corresponding to a zero-pressure boundary condition far away from the membrane. If the pressure is non-zero in only a finite region (e.g., a fluid or a gas contained between two walls with a finite spacing between them), the dependence on the difference in pressures in equations (3.49)–(3.52) guarantees that there is no curvature energy for an isotropic fluid system with  $\Pi_t = \Pi_{\ell}$  constant. (In this case, our expressions differ somewhat from those of [16, 20].) For a solid, however, the shear response of the system results in a non-zero bending modulus, even for an isotropic elastic medium [19]. We note that the combination  $k_{c0}$  and the saddle-splay modulus  $k$  are simply related to the moments of the pressure distribution of the flat membrane, while the bending modulus itself requires that the change in pressure due to curvature be calculated to linear order in  $H$ . For a given microscopic model (e.g. charged membranes, or polymers at an interface), this requires a solution of the density profile and the resulting free energy and pressure in the curved geometry. However,  $k$  and  $k_{c0}$  often scale in an identical manner with the microscopic parameters (e.g. charge density and membrane thickness); one can therefore find  $k$  quite simply and infer that  $k$  scales similarly. Finally, we observe that for membranes with stress-free boundaries at  $\zeta = \lambda$  ( $\Pi_{\ell}(\lambda, \lambda) = 0$  for all values of  $\lambda$ ), the expression for  $k$  simplifies.

Note that the elastic constants still depend on the area per molecule via their dependence on  $\lambda_0$  (see equation (3.38)). In section 3.2, we showed how one can include the fluctuations of the area  $\Sigma$  per molecule and obtain the effective bending energy together with a prediction of how the minimal value of  $\Sigma$  varies with the curvature of the film.

## 4. Curvature energy of solid thin films

### 4.1. Motivation

In this section, we discuss the curvature energy of thin solid films. They differ from liquid films in that solids have a finite shear modulus which enters into the

expressions for the bending constants. More importantly, solids can be bent coherently, preserving the topology of the lattice, or incoherently, resulting in the formation of defects. Based on [21] we show below that there is a critical value of the thickness (or alternatively of the curvature) at which dislocation lines (in the plane of the film) spontaneously form. Above this critical thickness, the dislocations tend to reduce the energy required to curve the thin film uniformly. Once the dislocations are formed, the bending energy of the film may be further reduced by an alignment of these defects into grain boundaries. The grain boundaries can take up all the curvature of the thin film in the form of sharp bends at the grain boundaries. Of course the problem of bending even a single plane of a crystalline material into a sphere requires *in-plane* defects. The number of these defects per layer, however, is independent of the film thickness; we therefore do not discuss them in this paper (but see, for example, [22]) since we focus on the scaling of the bending moduli with film thickness.

The theoretical treatment of the curvature of thin solid films is motivated by the observations of closed curved structures in the ‘fullerenes’ which consist of single layers or nested planes of carbon and other layered compounds, where the layers may be organized into nearly spherical [5], cylindrical [6] or even saddle-shaped [7] structures. While such structures are well known and understood in the context of the self-assembly of amphiphilic layers, their properties in the solid-state context are a subject of active research.

#### 4.2. Coherent–incoherent bending of solid thin films

The elastic theory of bending of coherent thin films dates back to the seventeenth century and has been well established since the nineteenth century (see Love [23] for a historical review). For the bending of a thin film (with normal  $\hat{\mathbf{z}}$ ), the solutions of the equilibrium equation for isotropic linear elastic materials [19] valid for small curvature are determined by the dependence of the strain on the location within the film. The strain is the derivative of the local displacement of the atoms, and on the neutral surface at  $z = 0$  the  $\hat{\mathbf{z}}$  component of the displacement is just the deformation  $\zeta(x, y)$  of the film away from being flat. For a thin film, with free surfaces, equilibrium requires that the normal stresses [19]  $\sigma_{xz} = \sigma_{xy} = \sigma_{zz}$  all vanish. This determines [19] that the  $\hat{\mathbf{x}}$  and  $\hat{\mathbf{y}}$  components of the displacement are equal to  $-z \partial \zeta / \partial x$  and  $-z \partial \zeta / \partial y$  respectively. Taking further derivatives of these displacements yields the strain tensor components

$$\epsilon_{xx} = -z \frac{\partial^2 \zeta}{\partial x^2}, \quad (4.1)$$

$$\epsilon_{yy} = -z \frac{\partial^2 \zeta}{\partial y^2}, \quad (4.2)$$

$$\epsilon_{xy} = -z \frac{\partial^2 \zeta}{\partial x \partial y}, \quad (4.3)$$

In a similar manner, one can show that  $\epsilon_{xz} = \epsilon_{yz} = 0$  while

$$\epsilon_{zz} = z \frac{\nu}{1 - \nu} \left( \frac{\partial^2 \zeta}{\partial x^2} + \frac{\partial^2 \zeta}{\partial y^2} \right). \quad (4.4)$$

Here,  $\nu$  is the Poisson ratio [19] which relates for an isotropic material the transverse compression to the longitudinal extension ( $\epsilon_{xx} = -\nu\epsilon_{zz}$ ) of a rod. This ratio is a function of the compressive and shear moduli and effectively varies between  $\frac{1}{2}$  and 0; in the case of negligible shear modulus  $\nu = \frac{1}{2}$  and it is zero when the shear modulus is comparable with the compressive modulus. These components of the strain tensor all change sign at the midplane,  $z = 0$ ; this is because the outer layers of the bent film are expanded while the inner layers are compressed.

The elastic energy  $u$ , per unit volume is given by [19]

$$u = \frac{E}{2(1+\nu)} \sum_{ik} \left( \epsilon_{ik}^2 + \frac{\nu}{1-2\nu} \epsilon_{ii}^2 \right), \quad (4.5)$$

where  $E$  is Young's modulus which is related to the shear modulus  $\mu$  by  $\mu = \frac{1}{2}E/(1+\nu)$ ; thus, when there is no shear modulus,  $E = 0$ . Using the formula for the elastic energy and the previously derived formulae for the strains, and integrating  $u$  over the thickness of the layer,  $-h/2 \leq z \leq h/2$ , one finds that the deformation free energy per unit area is given by the Helfrich form of equation (1.1) with the bending modulus  $k$  given by

$$k = \frac{Eh^3}{3(1-\nu^2)}. \quad (4.6)$$

The saddle-splay modulus  $\bar{k}$  is

$$\bar{k} = -\frac{Eh^3}{12(1+\nu)}. \quad (4.7)$$

For an isotropic material, both moduli vanish if there is no shear modulus. The Gaussian curvature modulus is negative, favouring isotropic curvatures. Both moduli scale with the cube of the film thickness; this is expected from the fact that the strains are linear in the distance from the neutral surface and the free energy is the integral of the square of the strain. It is also consistent with the expressions which relate the pressure distribution to the bending moduli as derived above.

To study the effects of incoherency and defects on the relaxation of the bending moduli, we consider the simple case of bending about a single axis, with curvature  $\kappa$  so that there is no Gaussian curvature. The origin of the coordinate system is again chosen to be in the centre of the plate and the strain is positive in the portion of the film which is expanded owing to the bend and is negative in the portion which is compressed. The strain energy per unit area associated with this elastic field is given by equation (4.6):

$$W_u = \frac{Eh^3\kappa^2}{24(1-\nu^2)}, \quad (4.8)$$

where  $h$  is the thickness of the plate. The subscript  $u$  indicates that this is the unrelaxed strain energy (see below).

This treatment assumes that all the layers bend coherently, preserving the topology of the solid. One can also imagine a situation where the layers have physically been decoupled from each other; they then would bend independently of each other and the total energy for the independent bending of  $h/a$  layers ( $a$  is the thickness of a single layer) is

$$W_r = \frac{Eha^2\kappa^2}{24(1-\nu^2)}. \quad (4.9)$$

This is of course equivalent to the bending energy of a smectic with decoupled layers. In this case, the strain energy is given by equation (4.8) with  $h$  replaced by the molecular layer thickness  $a$ ; the entire energy is then multiplied by the number  $h/a$  of layers in the film. Since each layer is independent, the strain and stress fields with each layer are given by the expressions listed above, with the origin of the coordinate system each time being chosen to lie in the centre of the layer. Therefore, several components of the stress and strain tensor fields are discontinuous through the thickness of the multilayer film. In fact, in this case, the individual layers are free to slip parallel to the interfaces. In a normal elastic continuum, such slipping is prevented by the compatibility conditions.

The presence of a slipping interface between the layers is predicated upon the assumption that the energy of the structure is independent of the relative translation state of the individual layers. This would be valid, for example, for amorphous solid sheets separated by thin layers of a lubricant. However, if the individual layers are ordered and interact with one another, then the energy of the system will be a function of the relative in-plane translation which is related to the presence of dislocation[24] defects. The discontinuity in the strains between the molecular layers may be described in terms of a network of dislocations between the layers. In this view, the energy associated with the discontinuity in strain at the interface is associated with the elastic energy of the dislocation network.

When slipping does occur, the presence of the structural energy associated with the discontinuity in strain at the interface suggests that the true bending energy is intermediate between those predicted by equations (4.8) and (4.9). In other words, the equilibrium slippage (or strain discontinuity) should be expected to be smaller when there are interactions between the molecular layers such that the bending energy is increased relative to that given by equation (4.9).

#### 4.3. Bending with dislocations

We begin by considering a uniformly curved layered material (the curvature itself inducing an in-plane strain in each layer) and consider the possibility that the in-plane strain state may differ from one layer to the next. This in-plane strain in each layer may be thought of in terms of changing the number of atoms in the layer which, if done at fixed layer area, could lead to an in-plane compressive or tensile stress.<sup>†</sup> These ‘extra’ atoms may come from matter transport within the film (figure 6) or from dislocations, as discussed in the next section. Since these ‘extra’ atoms create a strain which is not associated with an elastic deformation, this additional strain must be accounted for separately. Because the in-plane strain (and lattice constant) of each layer will differ when the number of atoms in a layer changes, two adjacent layers will be incoherent. (This incoherency, while relieving some of the elastic strain due to the bend, will be the source of the dislocation energy to be considered below).

---

<sup>†</sup> It is precisely this effect which is responsible for the fact that a thin liquid film has no bending energy (takes the shape of its container); molecules in the compressed region leave to join those in the expanded region of the film. In this manner, the film can bend and maintain constant local density.

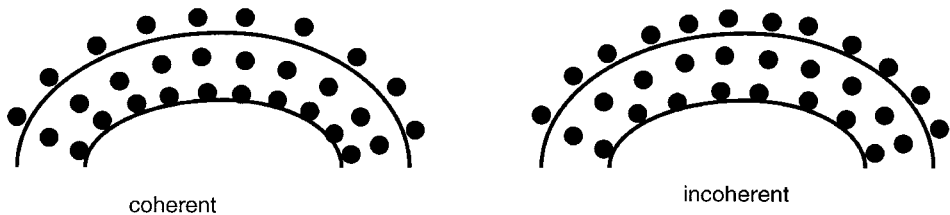


Figure 6. Schematic drawing of a coherently and an incoherently (deflected) bent thin film. The innermost layers of the coherently bent film are too compressed while the outermost layers are too expanded; this is because all layers must have the same number of atoms. The defect is created by removing atoms from the bottom layer (thus relieving the compression somewhat) and moving them to the top layer (thus relieving the expansion somewhat). This is a simple example of an interlayer dislocation in the film.

For simplicity, we consider bending of the sheet about a single axis ( $y$  axis), which produces the following strain distribution:

$$\epsilon_{xx} = -zK + n\epsilon_0, \quad (4.10)$$

where  $n\epsilon_0$  is the constant strain within layer  $n$  of the thin film (e.g. due to the dislocations). The layer index  $n = z/a$  where  $z$  is the location of the layer; at the neutral surface  $n = 0$ . The misfit strain discontinuity,  $\epsilon_0$ , between layers is assumed to be constant since the curvature is uniform. The strain  $\epsilon_{yy}$  in the  $\hat{y}$  direction is assumed to be zero and  $e_{zz} = -\epsilon_{xx}[v/(1-v)]$  because of the thin-film condition that the normal stress in the  $\hat{z}$  direction is zero, that is, plane stress. Applying Hooke's law, we find that the stresses are given by

$$\sigma_{xx}(x, n) = \frac{E}{1-\nu^2}(-Kz + n\epsilon_0) \quad (4.11)$$

and

$$\sigma_{yy}(z, n) = \nu\sigma_{xx}(z, n). \quad (4.12)$$

The resulting strain energy density is

$$w(z, n) = \frac{1}{2}\sigma_{ij}\epsilon_{ij} = \frac{E}{2(1-\nu^2)}(-Kz + n\epsilon_0)^2. \quad (4.13)$$

This result and all other elastic results in this and the following section are derived within the framework of linear elasticity where all stresses and strains are assumed to be small.

The total strain energy per unit length of cylinder, associated with equation (4.10), is obtained by integrating over the entire film which includes a sum over the index  $n$  which characterizes the strain due to the dislocations and an integral over the continuous variable  $z$  which specifies the bending strain and one finds [21] that

$$W_p = \frac{Eh}{24(1-\nu^2)} \left[ h^2 \left( \kappa - \frac{\epsilon_0}{a} \right)^2 + a\epsilon_0 \left( 2\kappa - \frac{\epsilon_0}{a} \right) \right], \quad (4.14)$$

where the subscript  $p$  indicates that the strain energy is partially relaxed. If the misfit strain discontinuity  $\epsilon_0$  is zero, then equation (4.14) reduces to equation (4.8), that is the unrelaxed bending energy of coherent films reduces to the relaxed strain energy

of incoherent films. In the limit that  $\epsilon_0 = Ka$ , equation (4.14) reduces to the relaxed strain energy, that is equation (4.9).

This result may be used to reinterpret the nature of the relaxation associated with the strain jump between layers. In uniform bending, the midplane of the film remains unstrained and is referred to as the neutral plane. If there is no strain discontinuity at the interface between layers, then the strain  $\epsilon_{xx}$  at the midplane of each layer grows linearly with increasing distance from the neutral plane of the film. Subtracting  $n\epsilon_0 = naK$  from the bending strain of layer  $n$  reduces the overall strain in layer  $n$  such that the strain on the midplane of layer  $n$  is zero, that is, it is a neutral plane. Either increasing or decreasing  $\epsilon_0$  from the value  $aK$  will increase the strain energy in the layer. To minimize the total energy, one must consider both the bending energy  $W_p$  and the energy of the interface between molecular layers associated with the translation of each layer with respect to its neighbouring layers (i.e. the discommensuration or dislocation network energy), as shown in the next section.

#### 4.4. Dislocations

Edge dislocations with Burgers vectors in the  $\hat{x}$  direction ( $b_x$ ) and line direction parallel to  $\hat{y}$  can relax the stress caused by the curvature  $\kappa$  [25, 26]. This relaxation is attributable to the fact that a spatially uniform array of edge dislocations of density†  $\rho$  [32] results in a lattice curvature given by  $\rho b_x$  [27]. The curvature that produces a stress is thus the difference between the lattice curvature and the macroscopic curvature. The stress in a curved crystal with a uniform density of dislocations is thus [26]

$$\sigma_{xx}(z) = \frac{Ez}{1-\nu^2}(\rho b_x - \kappa). \quad (4.15)$$

Comparing this result with the stress derived from equation (4.10) shows that  $\epsilon_0 = 1/\rho ab_x$ . Rewriting the partially relaxed bending energy equation (4.14) in terms of the normalized dislocation density  $\rho' = \rho b_x$ , we obtain the following energy per unit area of the curved crystal:

$$W_p = \frac{Eha^2}{24(1-\nu^2)} \left\{ \rho'^2 \left[ \left( \frac{h}{a} \right)^2 - 1 \right] - 2\rho'\kappa \left[ \left( \frac{h}{a} \right)^2 - 1 \right] + \kappa^2 \left( \frac{h}{a} \right)^2 \right\}. \quad (4.16)$$

The energy per unit length of an edge dislocation in an isotropic solid is given by

$$w_\perp = \frac{Eb^2}{8\pi(1-\nu^2)} \ln \left( \frac{R}{r_0} \right), \quad (4.17)$$

where  $b$  is the Burgers vector of the dislocation and  $r_0$  is the dislocation core cut-off parameter which is of order of an atomic dimension. The outer cut-off parameter  $R$  is typically assigned the value of half the spacing between dislocations and accounts for the screening of the stress field of each dislocation by those of the other dislocations in the solid. The elastic field of a dislocation in a film is complicated by the fact that the free surfaces introduce image-like terms into the elastic field. If a dislocation is very close to the free surface, it may be closer to its image than to the other dislocations within the film. In this case, the outer cut-off parameter  $R$  is

---

† The units of  $\rho$  are  $(\text{length})^{-2}$ ; the dislocation density represents the number of dislocation line lengths per unit volume which has an overall dimension of an inverse area.

approximately equal to the distance between the dislocation and the surface. In a thin film, this distance is of the order of the film thickness,  $h$ . For simplicity, we consider<sup>†</sup> the case where the density of dislocations is small so that  $h \ll \rho^{-1/2}$ .

The total strain energy per unit area associated with a density  $\rho$  of dislocations (line length per unit volume) in a film of thickness  $h$  may be approximated as

$$W_{\perp} = \frac{Eb^2 h \rho}{8\pi(1 - \nu^2)} \ln \left( \frac{h}{r_0} \right). \quad (4.18)$$

We note that in all cases,  $h/2$  must be less than the radius of curvature of the crystal in order to ensure that two sections of the surface do not cross. Since the maximum dislocation density is equal to  $\kappa/b$ , the large- $h$  limit is valid when  $2(\rho b)^{-1} \gg h \gg \rho^{-1/2}$ .

The total energy per unit area of the system is the sum of the dislocation and bending energy:  $W = W_p + W_{\perp}$ . When the solid is thin compared with the spacing between dislocations ( $h \ll \rho^{-1/2}$ ), the total energy is given by

$$W = \frac{Eh^3}{24(1 - \nu^2)} \left\{ \alpha \rho'^2 - \rho' \left[ 2\alpha\kappa - \frac{3b}{\pi h^2} \ln \left( \frac{h}{r_0} \right) \right] + \kappa^2 \right\} \quad (4.19)$$

where  $\alpha = 1 - (a/h)^2$ . The energy is a quadratic function of the dislocation density  $\rho' = \rho b$  and has a minimum corresponding to positive  $\rho'$  for all  $\kappa$  greater than a critical value  $\kappa_c$ :

$$\kappa_c = \frac{3b}{2\pi\alpha h^2} \ln \left( \frac{h}{r_0} \right). \quad (4.20)$$

We can minimize  $W$  with respect to  $\rho'$  in order to determine the equilibrium dislocation density  $\rho'^*$  and find that  $\rho'^* = 0$  when  $\kappa < \kappa_c$ . For values of the curvature greater than the critical curvature ( $\kappa > \kappa_c$ ) the minimization results in a finite value of the dislocation density and  $\rho'^* = \kappa - \kappa_c$ .

The equilibrium total energy, is given by the following simple relation:

$$W = \frac{Eh^3}{24(1 - \nu^2)} \kappa^2 \quad (4.21)$$

when  $\kappa < \kappa_c$  and

$$W = \frac{Eh^3}{24(1 - \nu^2)} [\kappa^2 - \alpha(\kappa - \kappa_c)^2] \quad (4.22)$$

when  $\kappa > \kappa_c$ . Since the atomic size  $a$  is usually much smaller than the thickness  $h$ ,  $\alpha$  is approximately unity and the energy  $\alpha$  is approximately linear in  $\kappa$  when  $\kappa > \kappa_c$ . This linear behaviour for the case where there are an equilibrium number of dislocations in the film is in marked contrast with the usual quadratic dependence of the bending energy on the curvature in the dislocation-free case.

These results show that the number of spontaneously generated dislocations is zero when the curvature is less than the critical curvature  $\kappa_c$ . As the curvature is increased beyond  $\kappa_c$ , the density of dislocations increases linearly. For the isotropic system consider here, the critical curvature  $\kappa_c$  is determined primarily by the

---

<sup>†</sup> This is completely appropriate in the region near the transition from no dislocations to curvature induced dislocations where  $\rho$  increases from zero. The case where the thickness is small compared with the spacing between dislocations is outlined in [21]. In this case, the equilibrium density of dislocations is proportional to the curvature with a term that is logarithmic in the curvature.



thickness of the film. The thinner the crystal, the larger is the critical curvature; thin crystals, where the bare curvature modulus is smaller, are therefore more likely to be dislocation free than thick crystals. (For anisotropic systems,  $\kappa_c$  also depends on the ratio of the in-plane to the interplanar shear elastic constants, as shown below.) Since the transition from a dislocation-free to a dislocated crystal with increasing curvature occurs at zero dislocation density, the dislocation density is continuous while its first derivative with respect to curvature is not. Therefore, this acts like a second-order phase transition in curvature. For all reasonable values of the physical parameters, the condition  $h \ll \rho^{-1/2}$  is satisfied at the transition. The case of large dislocation density or small thickness where the condition  $h \ll \rho^{-1/2}$  is not satisfied is examined in [21].

The transition from an undislocated to a dislocated crystal may also be analysed in terms of a critical thickness instead of a critical curvature. For fixed curvature,  $\kappa_c$  decreases with increasing film thickness as  $1/h^2$ . Therefore, for any fixed positive curvature an initially dislocation-free film will become dislocated at a thickness  $h = h_c$ , where  $h_c$  is given by the solution of  $h_c^2 = 3b \ln(h_c/r_0)/2\pi\alpha\kappa$ . The concept of a critical thickness for the relaxation of stresses is familiar from its application to the case of a misfitting heteroepitaxial film on a substrate [28].

This prediction of a transition from a dislocation-free state to one with a thermodynamic number of dislocations which relieve the bending energy may be useful in understanding why some (usually thin) nested fullerenes grow with a fairly uniform spherical or cylindrical geometry; thin nested fullerenes have high critical curvatures  $\kappa_c$  and one expects them to grow relatively dislocation free. On the other hand, thicker structures have a much smaller critical curvature for dislocation formation and one expects [29] them to grow with the intrinsic formation of grain boundaries or polygonalized morphologies; dislocations tend to organize themselves into grain boundaries. Recent observations [29] seem to show that thin nested fullerenes tend to be grain boundary free and to show spherically symmetric morphologies, in contrast with thicker systems.

#### 4.5. Bending of anisotropic solid films

In many cases of experimental interest, including the fullerene materials, the curved structures occur in anisotropic layered solids that typically have strong covalent bonds in the plane and weaker van der Waals attractive bonding between layers. The theory developed above can be generalized [19, 21, 30] to the case of a film which is isotropic in the plane but with different interplanar bonding; this is equivalent to the case of hexagonal symmetry with the  $c$  axis oriented normal to the surface of the film. The bending and Gaussian bending moduli are related to the elastic constants  $C_{\alpha\beta\gamma\delta}$  [19] via

$$k = \frac{h^3}{3} \left( C_{xxxx} - \frac{C_{xxzz}^2}{C_{zzzz}} \right), \quad (4.23)$$

$$\bar{k} = \frac{h^3}{3} (C_{xxyy} - C_{xxxx}) = -2C_{xyxy}. \quad (4.24)$$

In comparison with the isotropic case, the bending modulus for the anisotropic material depends on the difference between the in-plane compressional modulus  $C_{xxxx}$  and a term related to the Poisson ratio that couples in-plane and out-of-plane deformations. This term always reduces the bending modulus of the material by

providing an extra dimension of mechanical relaxation that is not present in strictly two-dimensional systems such as amphiphilic monolayers. The Gaussian curvature modulus  $k$  depends only on the in-plane shear modulus, implying that materials with very low in-plane shear moduli may have very small resistance for forming saddle-shaped structures. For graphite, the measurements of Blakeslee *et al.* [31] imply that  $k_v = k/(a^3/3) \approx 105 \times 10^{11} \text{ dyn cm}^{-2}$  and the ratio  $|k|/k \approx 0.8$ . In this material, as in other van der Waals layered solids, the in-plane stretching constant  $C_{xxxx}$  dominates the elasticity. Equation (4.14) for the bending energy remains the same with the factor  $E/(2(1-\nu^2))$  replaced by  $k_v$ .

The energy of a dislocation in an anisotropic elastic material can be written [32]

$$W_{\perp} = \frac{Jb^2}{4\pi} \ln \left( \frac{R}{r_0} \right), \quad (4.25)$$

where  $J$  depends on several components of the elastic constant tensor. In the case when the interplanar bonding is weak such that the elastic constants with a  $z$  component are all small,

$$J \approx (C_{xxxx}C_{xzxz})^{1/2}. \quad (4.26)$$

The strong dependence of  $J$  on the anisotropy is not surprising since the dislocations of interest arise from removing atoms from the compressed (inner) layers and transferring them to the expanded (outer) layers; they thus involve misfit between the planes and the weak shear modulus between layers has a significant effect on the dislocation energy. Using the values of the elastic constants for graphite, it can be shown that this results in a lower energy for a dislocation of about a factor of five, compared with an isotropic material, approximated in these layered systems by measurements in polycrystalline systems [21].

As in the previous section, one can calculate the critical curvature at which dislocations spontaneously form and one finds for the anisotropic case that

$$\kappa_c = -\frac{3bJ}{2\pi\alpha h^2 k_v} \ln \left( \frac{h}{r_0} \right) \quad (4.27)$$

where again  $k_v = k/(a^3/3)$  and  $a$  is the thickness of a layer. This is identical with the result found in the isotropic case but with a reduction factor of  $J/k_v$ ; in graphite,  $J/k_v$  is typically 0.06. The factor  $J/k_v$  may be small in a layered material such as graphite, thus significantly reducing the value of the critical curvature  $\kappa_c$ . In the isotropic limit,  $J = k_v/2 = E/[2(1-\nu^2)]$  and we recover the previous results. The physical origin of the anisotropy factor  $J/k_v$  in the expression for  $\kappa_c$  may be traced to the fact that the dislocations relieve the in-plane strains, whose energy cost is related to  $k_v$ , while the energy cost of creating a dislocation (arising from its long-range strain field) is related to the interplanar shear modulus through  $J$ . In highly anisotropic materials, the critical value of the curvature at which the dislocations are spontaneously generated can be very low, owing to the low energy cost of creating dislocations relative to curvature. Again, there will be a second-order type of transition from the dislocation-free coherent crystal to one with a finite number of dislocations as the curvature exceeds the critical curvature  $\kappa_c$ , which is now controlled by both the film thickness and the anisotropy. Similarly, the expression for the critical thickness will be reduced by a factor of  $J/k_v$  and one would expect departures from sphericity (due to the interactions between dislocations and the

formation of some type of grain-boundary structure) to occur at small thickness or curvatures.

## 5. Microscopic models

In this section, we supplement the phenomenological discussion of curvature elasticity by more microscopic models. The discussion of these models is not meant to be exhaustive, but rather illustrative of the fact that many different microscopic scenarios all result in the curvature elastic energy (per unit area) of a surfactant monolayer. We begin with a review of a very simple ball-and-spring model of surfactant molecules and then proceed to use the relation between the pressure distribution and the bending elastic constants derived above to estimate the moduli in charged films and in monolayers composed of block copolymers.

### 5.1. Ball-and-spring models

The simplest models of surfactant molecules that give rise to the curvature elastic energy [33] treat the molecules as (asymmetric) dumb-bells with the polar head groups and the chains each idealized as a point particle, attached by a rigid rod. The heads of different molecules are attached to each other by springs as are the chains. While this model yields expressions for the elastic constants in terms of the spring constants and equilibrium spring lengths which are physically reasonable, we use a slightly different formulation in which the surfactant chains are treated not as point-like entities but as spring-like molecules themselves. This provides a simple example for the treatment of block copolymer surfactants.

As a simple microscopic model that will allow some more physical insight into the meaning of the curvature elastic moduli, we consider a monolayer of chains that we model as springs with a spring constant  $k_s$  and with an equilibrium spring length  $\ell_s$ . We denote the actual (stretched or compressed) length of the spring by  $\ell$  (figure 7). We assume that the chains form an incompressible ‘melt’ with no penetration of solvent into the chains. Their free energy is proportional only to the stretch of the springs; such a picture is applicable to polymeric molecules that pack incompressibly but are stretched near an interface, so that the free energy cost for deformations arises from stretching. The area per chain at the interface is assumed to be fixed at a value  $\Sigma_0$ ; in reality, this value is determined by the interactions that act on the polar head groups and our simple model assumes that these interactions are much stronger than the chain stretching energies, so that the optimal head area  $\Sigma_0$ , determined by the interactions in the polar layer, is not affected by the chains. The energy per chain is thus

$$f = \frac{1}{2}k_s(\ell - \ell_s)^2, \quad (5.1)$$

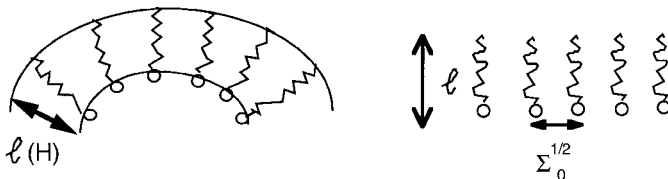


Figure 7. Model of a thin film composed of springlike molecules whose spring length  $\ell(H)$  depends on the mean curvature  $H$ . The area per molecule is  $\Sigma_0$  and  $\ell$  is the spring length in the flat film.

and the incompressibility of the chains implies that the volume occupied by the layer is constant. For a flat layer, this would be written  $\Sigma_0 \ell = v_0$  where  $v_0$  is the molecular volume. For a curved layer, the volume occupied by the chains depends on the curvature. The volume per molecule is

$$v_0 = \Sigma_0 \ell \left( 1 + \ell H + \frac{1}{3} \ell^2 K \right), \quad (5.2)$$

where  $H$  and  $K$  are the mean and Gaussian curvatures respectively. (This formula is based on the integral of the expression for the area of a parallel surface, discussed in section 2.1. and in [2].)

Thus, the incompressibility condition relates the layer thickness  $\ell$  and the area  $\Sigma_0$  per molecule. For fixed  $\Sigma_0$ , this determines the free energy as a function of curvature obtained by solving equation (5.2) for  $\ell$  and using this value for  $\ell$  in equation (5.1). The result is

$$\ell = \ell_0 + \ell_1 H + \ell_2 H^2 + \ell_3 K, \quad (5.3)$$

where  $\ell_0 = v_0/\Sigma_0$ ,  $\ell_1 = -\ell_0^2$ ,  $\ell_2 = 2\ell_0^3$  and  $\ell_3 = -\ell_0^3/3$ . Note that, for a flat layer, the incompressibility constraint determines the layer thickness to be equal to  $v_0/\Sigma_0$ ; in general, this will not be equal to the thickness  $\ell_s$  which minimizes the chain stretching energy. The flat layer is not, in general, the minimal energy state since the imposed thickness  $\ell_0$  is not identical with the preferred thickness  $\ell_s$ . Only when these two lengths are equal is the flat monolayer relieved of the frustration induced by the mismatch of these two lengths. The layer will then tend to bend; a spontaneous curvature will be induced so that the resulting thickness more closely matches  $\ell_s$ .

Using the incompressibility relation, we find that the elastic energy per chain is given to lowest order by

$$f = \frac{k_s \ell_0^4}{2} \left( (H - c_0)^2 - \frac{2c_0 \ell_0}{3} K \right), \quad (5.4)$$

where a higher-order term in  $c_0 \ell_0 H^2$  has been neglected. The spontaneous curvature  $c_0$  is related to the difference between the chain length,  $\ell_0$  dictated by the molecular volume conservation and the head packing, and the chain length  $\ell_s$ , preferred by the chain stretching energy:

$$c_0 = \frac{\ell_0 - \ell_s}{\ell_0^2}. \quad (5.5)$$

Equation (5.4) is equivalent to the ‘Helfrich’ form of the curvature free energy (equation (1.1)) by a simple transformation that converts from energy per molecule to energy per unit area. The bending modulus (coefficient of  $H^2$ ) and the saddle-splay modulus (coefficient of  $K$ ) both increase as a power of the chain length. Of course, the spring constant  $k_s$  also depends on the equilibrium spring length  $\ell_s$ ; a simple polymeric analogy yields in the limit of small curvatures,  $k_s \sim 1/\ell_s \approx 1/\ell_0$ . In that case, the bending modulus  $k \sim \ell_s^3$ . This variation of the bending modulus with the cube of the thickness is also characteristic of a bent solid elastic plate as discussed above and in [19].

Recent estimates of the curvature elastic constants from analysis of neutron scattering on fluctuating microemulsion droplets and from surface tension measurements [34] have shown that increasing the chain length of the surfactants from C<sub>8</sub> to C<sub>10</sub> results in an increase in the elastic constant by a factor of two, while

increasing from  $C_8$  to  $C_{12}$  results in an increase of 3.6 in the elastic constant. These very nonlinear dependences of the bending moduli on the chain length are consistent with the predictions mentioned above.

The quantity  $c_0$  is the spontaneous curvature of the membrane, which this model endows with a simple physical meaning: When the imposed head area  $\Sigma_0$  is larger than the optimal area  $v_0/\ell_s$  dictated by the chain packing, the preferred curvature is negative; the system prefers to pack with the heads on the ‘outside’. Note that the free energy of the curved interface is lower than that of the flat interface; the system accommodates part of the strain induced by the mismatch between the heads and chains by bending.

An interesting result of this particular model is that the saddle-splay or Gaussian curvature modulus  $k$  is proportional to the spontaneous curvature. As discussed above (see equation (2.21)), this depends on the location of the plane of curvature which in this calculation is taken quite naturally at the polar head surface. For example, if the plane of curvature is taken to be at  $\ell/3$  above the polar head surface, the resulting Gaussian modulus vanishes. This choice also modifies the effective bending constant.

As discussed previously, this expression for the bending energy is found for a fixed value of the area  $\Sigma$  per head. The physically relevant relaxed bending energy of the system is obtained by minimizing the total free energy with respect to  $\Sigma$  and recalculating the bending moduli as shown in section 3.2.

## 5.2. Charged head-group contributions to curvature elasticity

### 5.2.1. Charged surfaces and counterions

The previous section indicated how, in a very simple model, one can account for the contribution of the hydrocarbon chains in the bending modulus of a surfactant monolayer. The heads were modelled as an incompressible two-dimensional fluid which enforced a specific packing area. In this section, we consider the contribution to the bending modulus from the polar heads; in general, this requires a detailed molecular calculation which takes into account their packing and interactions. However, we focus here on the more universal aspects of these interactions and consider the case where the surface of polar groups can be idealized by a sheet of molecules with fixed charge with counterions distributed in the water. We then find the energy to bend such a sheet (allowing the counterions to respond) and use the relationship between the pressure distribution and the bending moduli to study the scaling of  $k$  and  $\bar{k}$  as a function of the charge density and the distance between layers.

Electrostatic interactions are important, and often dominant, in systems where there is some separation between charged groups and thus some finite-range internal electric field. For example, some surfactant molecules have a fixed charge, which remains attached to the molecule, and mobile counterions, which are solvated by polar solvents. In the  $\text{NaSO}_3$  polar groups, the positively charged Na is mobile while the  $\text{SO}_3$  group is the negative fixed charge (figure 8). Usually the interactions between the different layers are repulsive (except possibly when the distances between the interfaces become of order of a molecular size). In describing these systems, one speaks of the fixed charge at the surface of polar heads and the delocalized or mobile counterion that lowers its free energy through the entropy it gains by being in solution. The problem of interest is to find the spatial distribution of counterions around the surface of fixed charges. The Coulomb attractions tend to *bind* the counterions close to this interface while their entropy of mixing with the solvent



electrostatic energy of both the mobile and the fixed charges as well as the ideal gas entropy of the mobile charges. The electrostatic potential  $\psi(\mathbf{r})$  is related to the mobile charge density  $n(\mathbf{r})$  by

$$\psi(\mathbf{r}) = \int \frac{n(\mathbf{r}')}{|\mathbf{r} - \mathbf{r}'|} d\mathbf{r}'. \quad (5.6)$$

Minimization of the total free energy [2] yields the Poisson–Boltzmann equation for the potential:

$$\nabla^2 \psi(\mathbf{r}) = -4\pi\epsilon_0(\mathbf{r}), \quad (5.7)$$

$$n(\mathbf{r}) = n_0 \exp[-\ell\psi(\mathbf{r})], \quad (5.8)$$

where  $\ell = e^2/\epsilon k_B T$  is the Bjerrum length and is a measure of the ratio of the electrostatic energy (which is minimal when all the counterions are at the surface of fixed charge) to the entropy (which is maximal when the counterions are uniformly distributed in the solvent). The constant  $n_0$  is determined from charge conservation; when the mobile charge density is integrated over the entire volume, the total number of charges must balance the number of fixed charges on the polar head group surface. The exponential factor in equation (5.8) comes from the Boltzmann distribution of the counterions whose energy is determined by the potential  $\psi$ ; this simple relationship between the charge and the potential is only true within the ideal-gas approximation for the counterion entropy and will be modified if one takes finite ion size and excluded volume effects into account.

We now consider a single planar interface at position  $z = 0$  with a uniform fixed charge density per unit area  $\sigma_0$ . Defining

$$\phi = \ell\psi, \quad (5.9)$$

we have from equations (5.6) and (5.7)

$$\nabla^2 \phi = -4\pi\epsilon_0[n_0 \exp(-\phi)]. \quad (5.10)$$

The quantity  $n_0$  is determined from the conservation law

$$n_0 \int_{-\infty}^{\infty} dz \exp(-\phi) = \sigma_0. \quad (5.11)$$

The solution of equation (5.10), whose charge density decays to zero as  $z \rightarrow \infty$ , is

$$\phi = 2 \log [(|z| + \lambda)(2\pi\epsilon_0\ell)^{1/2}], \quad (5.12)$$

$$n(z) = \frac{1}{2\pi\ell} \frac{1}{(|z| + \lambda)^2}, \quad (5.13)$$

where the characteristic length

$$\lambda = \frac{1}{\pi\ell\sigma_0}. \quad (5.14)$$

The charge density falls off slowly at large distances; however, most of the charge is localized in a layer of width  $\lambda$ , which tends to zero as the fixed-charge density  $\sigma$  goes to infinity.

The charge density surrounding a single layer is extremely long ranged and this can be problematic when calculating the bending moduli which are moments of this

distribution. We therefore consider the case of a lamellar stack of charged surfaces with a repeat distance  $2D$  where the counterions in the solvent are between the layers of fixed charge. A calculation similar to that for a single layer shows that the charge density is given by

$$n(z) = \frac{n_0}{\cos^2(k_0 z)}, \quad (5.15)$$

where charge conservation determines that

$$k_0 D \tan(k_0 D) = \pi \ell \sigma_0 D. \quad (5.16)$$

There are two interesting limits to this problem depending on the charge density  $\sigma_0$  relative to  $1/\ell D$ .

- (i) *Ideal-gas limit.* In the limit of low charge density,  $D\ell\sigma_0 \ll 1$ ,  $k_0 D \ll 1$ , so that  $n \approx \sigma_0/2D$  and is only weakly dependent on  $z$ . This is the ideal-gas limit where the counterions are nearly uniformly distributed between the two layers.
- (ii) *High-charge-density limit.* In the limit of high charge density,  $D\ell\sigma_0 \gg 1$  (large separations and high charge densities),  $k_0 D \approx \pi/2$  and  $n_0 \ell \sim 1/D^2$ . For a uniform charge distribution,  $n_0 \approx \sigma_0/2D$ ; so this result tells us that the charge at the midplane,  $z = 0$ , is smaller than that of a uniform distribution by an additional factor of  $1/\ell\sigma_0 D$ . As the spacing between the interfaces is made larger, the *ratio* of the charge at the midplane to a uniform charge distribution decreases. This result is strongly geometry dependent. These results suggest that one can think of an effective ‘fixed’ charge  $Z^*$  given by the actual fixed charge ( $Z = \sigma_0 A$ , where  $A$  is the area of the sheet) minus the charge of those counterions localized near the fixed charges. For distances much greater than  $\lambda$ , the system approximately behaves as if the effective mobile charge

$$Z^* \approx Z \left( \frac{1}{\ell \sigma_0 D} \right) \quad (5.17)$$

of counterions was uniformly distributed in the space between the effective fixed charges. Thus, the long-distance properties determined by these interactions are strongly influenced by the reduction of the Coulomb interactions by these effects.

When the system contains additional salt, the long-range interaction discussed here is screened by the salt ions and the potentials and charge distributions fall off exponentially as a function of distance from the plane of fixed charge. The decay or screening length  $\lambda_s$  is related to the salt concentration  $n_s$  by  $\lambda_s = 1/(8\pi n_s \ell)^{1/2}$ .

### 5.2.2. Bending of charged layers

The discussion in the previous section summarized the basic physics of flat charged layers. In order to calculate the changes in energy of these layers (which is most sensitive to the spatial distribution of the counterions), one must explicitly solve the Poisson–Boltzmann equation for the curved geometry. Detailed theories of these effects have been presented in [11–14]. Here we use dimensional considerations to relate the bending constants to the electrostatic properties of the charged polar head groups, the counterions, and any electrolyte that may be present in the water.



We begin by recalling equations (3.49)–(3.52) which relate the bending moduli to the pressure distribution. In the case of charged layers with counterions distributed inhomogeneously in the water, the relevant pressure distribution is that of the counterion ‘gas’. We note that the bending constants scale as the product of the transverse pressure difference and the cube of a characteristic length which characterizes the thickness over which the transverse pressure difference is significant.

From quite general considerations [2], the transverse pressure  $\Pi_t$  of the gas of counterions in a system of charged monolayers is equal to the product of  $k_B T$  (where  $T$  is the temperature) and the difference between twice the charge density  $n(z)$  at a given point and the midplane between layers which is taken at  $z = 0$ :

$$\Pi_t = k_B T [2n(z) - n(0)]. \quad (5.18)$$

Although this resembles the ideal-gas result, one must remember that the charge distribution of the counterions in solution is inhomogeneous.

Using the expressions for the charge density derived in the previous section we see that the charge density at the surface of fixed charge, where the bending occurs and where the pressure difference is largest, scales as  $n(0) \sim 1/\lambda^2 l$ . The pressure at that surface is the product of  $k_B T n(0) \sim k_B T / \lambda^2 l$ . On the other hand, the pressure difference at a distance  $d$  from the surface of fixed charge (the polar head groups) scales as  $k_B T n(d)$  and if  $d \gg \lambda$  this is proportional to  $k_B T / d^2 l$ . To determine the characteristic length scale over which this pressure is effective we consider three different cases:

- (i) the case of no added electrolyte, but where there is an array of charged sheets, as in a lamellar phase and the spacing between sheets  $d \ll \lambda$ ; this is relevant in the limit of very small surface charge densities which is sometimes termed the ideal-gas limit;
  - (ii) as in (i) but where the charge density is relatively high so that  $d \gg \lambda$ ;
  - (iii) the case of added electrolyte of concentration  $n_s$  where the relevant length scale is the screening length  $\lambda_s \sim 1/(n_s l)^{1/2}$ .
- (i) For an array of sheets in the case of no electrolyte and weak surface charge ( $d \ll \lambda$ ), the length scale over which the pressure difference is significant is the entire distance between the sheets  $d$  while the pressure difference is proportional to  $k_B T / \lambda^2 l$ . We thus estimate that the bending modulus scales as

$$k \sim k_B T \frac{d^3}{\lambda^2 l}, \quad (5.19)$$

Using the expressions for  $l$  and  $\lambda$ , we see that the bending modulus is proportional to the strength of the Coulomb interaction energy; if, in this nearly ideal-gas limit of weak surface charge, the counterions were distributed completely uniformly (with absolutely no effect of the electrostatic interactions), the bending modulus would vanish, as discussed previously.

- (ii) For an array of sheets in the case of no electrolyte and strong surface charge ( $d \gg \lambda$ ), the length scale over which the pressure difference is significant is still  $d$ , but the pressure over most of that region is better estimated by  $k_B T / d^2 l$ . The bending modulus thus scales as

$$k \sim k_B T \frac{d}{l}. \quad (5.20)$$

Here we see that bending modulus is indeed proportional to temperature with an additional factor of  $k_B T / e^2$  which accounts for the electrostatics. This proportionality indicates the role of the entropy in determining the spatial distribution of the counterions; if the entropy were ignored, in this strong surface charge limit, all the counterions would collapse onto the fixed charge and there would no resulting contribution to the bending energy.

- (iii) For the case of added electrolyte, the relevant length scale where the pressure different is effective is the screening length  $\lambda_s$  and this screening length plays the role of  $d$  in cases (i) and (ii). Thus, for example, in the weak surface charge limit

$$k \sim k_B T \frac{\lambda_s^3}{\lambda^2 l}. \quad (5.21)$$

Here the screening length plays the role of the interlayer spacing  $d$  in case (i).

Typical values of  $\lambda$  (for unit charge per polar group) and  $l$  are of the order of 10 Å. We thus see that the electrostatic contributions to the bending energies can be significant compared with  $k_B T$  when either the interlayer spacing (for systems with no added electrolyte) or the screening length (for systems with added salt) are large compared with  $\lambda$  or  $l$ . When the screening is strong, the screening length is small, and the contributions to the bending energy can be negligible. On the other hand, for the case of no added electrolyte and a large interlayer spacing, the electrostatic contribution to the bending modulus can be quite significant. The exact value of  $k$  depends, of course, on numerical factors not given by our scaling arguments. These factors have been discussed in [11–14] for the various cases and sometimes give rather small numerical pre-factors of the order of  $\frac{1}{10}$  or smaller. Furthermore, the sign of the saddle-splay modulus  $k$  is negative; this tends to favour spherical topologies over saddle-like or flat structures. The spherical shape for the surface of polar heads allows for more volume and thus relatively greater entropy of the counterions [35, 36]. In addition, as noted in the previous section and as we emphasize in the following section, the chain contributions to the bending energy scale with powers of the chain length. Thus, crudely speaking, one must compare the interlayer spacing or the screening length for the charged head-group electrostatic contributions with the chain length for the tail contributions to determine whether the bending modulus is dominated by the heads or chains.

Finally, we note that these results depend parametrically on the packing density of the fixed charge and hence of the polar head groups; here we have taken this quantity to be constant. In practice, the free energy should be further minimized with respect to fluctuations in the area per molecule; this results in a downwards renormalization of the bending modulus as we have previously shown in equation (3.7). To carry this out, one needs a particular model for the interactions of the polar group and the dependence of the total energy on the packing area per head.

### 5.3. Chain contributions to curvature elasticity

While the previous discussion of the electrostatic contribution to the bending energy is applicable to strongly charged systems, one expects that for non-ionic surfactants (or even zwitterionic surfactants where there is a permanent dipole

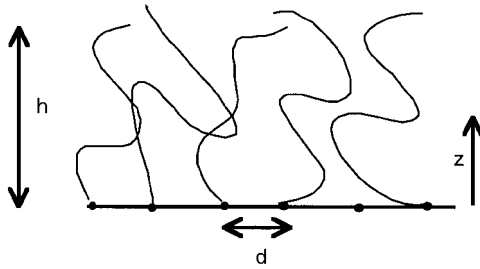


Figure 9. A polymeric brush of height  $h$  and where  $d$  is the spacing between the grafted ends.

moment of the polar head group, but no large spatial separation between the charges) the contributions of the hydrocarbon chains will dominate the bending modulus; the polar head groups will enter in providing packing constraints on the area  $\Sigma$  per molecule, but the bending response of the thin film will be mostly that of the tail region.

Detailed treatments of the response of both grafted polymer chains [15] and block copolymers [10, 37–39] to bending have been presented. Here, for simplicity, we use scaling arguments to relate the transverse pressure distribution in the polymeric layer to the bending moduli. As in the previous section, the bending modulus scales as the product of the transverse pressure difference and the cube of the relevant length scale. The transverse pressure itself scales as the free energy per unit volume.

### 5.3.1. Melt brush

The simplest case to treat is that of a ‘melt brush’ of chains with no penetration of the layer of chains by the hydrophobic solvent (figure 9). Using a simple Flory model [40], one writes the free energy  $F$  per chain as a function of the chain extent  $h$  as

$$F = \frac{3k_B T}{2} \frac{h^2}{Na^2}, \quad (5.22)$$

where  $a$  is the monomer size and where there are  $N$  monomers in the chain. This just represents the entropy cost of stretching a Gaussian chain. By conservation of chain segments, the product of the height and the area  $\Sigma$  per chain along the interface must obey  $h\Sigma = Na^3$ . The transverse pressure is just the free energy per unit volume:  $\Pi_t = F/\Sigma h$ . Using these relations, we find that the bending constant in the Helfrich representation scales as  $\Pi_t h^3$ . For the case of chains where the surface of curvature is measured at the chain end and not along the neutral surface and where the free energy is most conveniently expressed per chain, it is useful to define a bending constant  $k_c$ , associated with the free energy per chain and not the free energy per unit area; thus  $k_c = \Sigma k$  relates this modulus to the usual modulus  $k$ . A scaling analysis yields  $k_c \sim \Pi_t h^3 \Sigma$  and we find that

$$k_c \sim \frac{N^3}{\Sigma^4}. \quad (5.23)$$

For chains irreversibly grafted at the hydrophobic interface, this is as far as one can go in predicting the bending modulus as a function of polymerization index  $N$ , since

$N$  and  $\Sigma$  are independent. However, in the case of self-assembled chains, the area per chain adjusts itself to minimize the total free energy which includes both the chain stretching contribution and the interfacial energy  $\gamma\Sigma$  which represents the increase in the chain–water or chain–polar head contacts as the area per chain is increased. Minimizing the total free energy with respect to  $\Sigma$  determines the scaling of the equilibrium value of the chain packing  $\Sigma^*$  with  $N$  as

$$\Sigma^* \sim N^{1/3}. \quad (5.24)$$

Using this result in equation (5.23) we find that

$$k_c \sim N^{5/3}. \quad (5.25)$$

This is a considerably weaker dependence on  $N$  than the result for irreversibly grafted chains where  $k_c \sim N^3$ . The softening of the bending modulus is due to the relaxation of the free energy by the chains adjustment of their packing area  $\Sigma$ . A more detailed treatment of this problem [38] yielded similar scaling.

### 5.3.2. Swollen chains at an interface

We now consider a grafted polymer layer swollen by a good solvent. The polymer has an area  $\Sigma$  per molecule which at this point we regard as being fixed. The free energy [40] consists of two contributions: firstly the excluded volume interactions of the polymeric segments with each other which scales (in a good solvent) like  $v c(z)^2$ , where  $c(z)$  is the local concentration of monomers and  $v$  is the excluded volume per monomer; secondly the stretching energy of the chains which increases quadratically with the extent (distance from the grafting surface to the chain end) of each chain. The free energy per chain is thus written as

$$F = \Sigma k_B T \int_0^h dz \left( \frac{1}{2} v c(z)^2 + \frac{3z^2 c(z)}{2Na^2} \right), \quad (5.26)$$

where the coefficient of  $z^2$  in the stretching energy is a crude approximation that the probability of a chain end existing at a given value of  $z$  is proportional to the local average concentration  $c(z)$  of monomers. The balance of these two terms and a Lagrange multiplier term which constrains the conservation of chain segments yields [2, 41] a parabolic density profile [15, 41] with

$$c(z) = \frac{\eta}{v} \left[ 1 - \frac{1}{2\eta} \left( \frac{z}{Na} \right)^2 \right], \quad (5.27)$$

where  $N$  is the number of monomers in the chain and  $a$  is the monomer size. The dimensionless constant  $\eta$  scales as  $1/\Sigma^{2/3}$  and is independent of  $N$ . One can minimize the free energy with respect to the brush height  $h$ , and one finds that chains in the brush are stretched with an extent that scales linearly with  $N/\Sigma^{1/3}$ ; this differs considerably from the situation of free chains in good solvents where the chain extent scales as  $N^{1/2}$  without excluded volume and  $N^{3/5}$  if excluded volume interactions are taken into account. Thus the relevant length scale over which there is a significant transverse pressure difference scales linearly with  $N$  and we therefore expect the bending moduli to scale as  $N^3$  (since the pressure itself is a function of  $z/N$ ).

Using the same type of estimates as in the previous section, we find that the free energy scales as  $F \sim \Sigma \eta^2 h \sim N/\Sigma^{2/3}$ . The transverse pressure  $\Pi_t$  scales as  $F/\Sigma h$  and the bending constant  $k_c \sim \Sigma \Pi_t h^3$  thus scales as

$$k_c \sim \frac{Nh^2}{\Sigma^{2/3}} \sim \frac{N^3}{\Sigma^{4/3}}. \quad (5.28)$$

As before, this is the final result for irreversibly grafted chains. If the chains are, however, free to adjust their packing area, one must minimize the total free energy given by the sum of  $F$  and the surface tension term  $\gamma\Sigma$ . Doing this determines the equilibrium value of  $\Sigma^* \sim N^{3/5}$  and one then finds that

$$k_c \sim N^{11/5}. \quad (5.29)$$

A more sophisticated analysis given in [38, 42] indicates that  $F \sim N/\Sigma^{5/6}$  with all the other relationships remaining the same. Going through the same procedure yields

$$k_c \sim Nh^2/\Sigma^{5/6} \sim N^3/\Sigma^{3/2} \quad (5.30)$$

for the case of irreversibly grafted chains and

$$k_c \sim N^{24/11} \quad (5.31)$$

for the case of chains that are self-assembled and free to adjust their packing area on the interface. The numerical values of the scaling exponents are very close in both the simple and the more sophisticated treatments.

For completeness, we cite [38] the results for the bending moduli (in the formulation of the bending energy per chain given by  $k_c = \Sigma k$ ,  $k_c = \Sigma \bar{k}$ ) for the case of a block copolymer consisting of a total of  $N$  segments with identical persistence lengths and excluded volume parameters but where the A (B) block has  $N_A$  ( $N_B$ ) segments so that  $N = N_A + N_B$ . One can think of the A block as being the ‘head’ and the B block as the tail of this amphiphilic surfactant. We characterize the asymmetry of the ‘head’–‘tail’ packing by  $\epsilon = (N_B - N_A)/N$  and define the interfacial tension in units of  $k_B T$  between the water and oil as  $\gamma$ . We take all the microscopic parameters (persistence length and excluded volume) to scale with the same microscopic length  $a$ . The moduli and spontaneous curvature are then given for two different cases to lowest order in  $\epsilon$ , for small asymmetry (for more details see [38]).

- (1) For the case of a block copolymer in a good solvent,

$$k_c = 0.0881 k_B T \gamma^{9/11} N^{24/11}, \quad (5.32)$$

$$\bar{k}_c = -0.0499 k_B T \gamma^{9/11} N^{24/11}, \quad (5.33)$$

$$c_0 = \frac{3.853 \epsilon \gamma^{-2/11} N^{-9/11}}{a}. \quad (5.34)$$

- (2) For the case of a block copolymer melt (no penetration of the solvent into the block copolymer layers) the results are similar but with somewhat different scaling exponents:

$$k_c = 0.067 k_B T \gamma^{4/3} N^{5/3}, \quad (5.35)$$

$$\bar{k}_c = -0.053 k_B T \gamma^{4/3} N^{5/3}, \quad (5.36)$$

$$c_0 = \frac{2.134 \epsilon \gamma^{-1/3} N^{-2/3}}{a}. \quad (5.37)$$

These results provide us with a ‘microscopic’ model for a system of interacting chains which can be used to estimate the bending modulus from the first principles of the polymer statistics. It is interesting to note that the ratio,  $k_c/k_c$  of the Gaussian to bend moduli lies in the range from  $-0.56$  for the case of chains in good solvent to  $-0.79$  for a melt. These values are close to the value of  $-\frac{2}{3}$  predicted by the simple spring model discussed above. To apply the spring model to polymer one must take the preferred spring length  $\ell_s$  to be zero; the spontaneous curvature then scales as the chain length  $1/\ell_0$  and the product of  $c_0\ell_0$  is of the order of unity. The polymer theory can be extended to treat the case of mixed chains and to provide insight into how the interactions between long and short chains can dramatically modify the bending moduli; these ideas have been used to suggest a mechanism for spontaneous vesicle formation in mixed-chain systems [17].

## 6. Role of thermal fluctuations and inhomogeneities

As we have seen in the discussion of the relaxation of the area per molecule at the interface, additional degrees of freedom over and above the interface curvature tend to lower the effective bending modulus [43]. Another effect that has been only recently discussed [44] involves the orientable anisotropic defects in possibly changing the sign of the saddle-splay modulus  $k$  from its usual negative value. This can occur as the defects cooperatively orient; if they couple to the membrane in an appropriate manner, they can strongly prefer saddle-shaped structures.

In this section we consider two degrees of freedom that can soften the bending modulus  $k$ . Firstly thermal fluctuations soften the modulus at long distances in a manner that depends logarithmically on the length scale. The renormalization and softening of the bending modulus at long length scales have important implications for the structure and phase behaviour of such systems such as microemulsions [45, 46] and the size distribution of equilibrium vesicles [47, 48]. For example, the Boltzmann factor governing the vesicle distribution has as its argument a term in the bending free energy that is logarithmic in the globule size. The effect of a logarithmic term in the Boltzmann exponential results in a power-law contribution to the vesicle size distribution whose exponent depends on the coefficient of this logarithmic term. Secondly mixing of different amphiphiles [49] (and, in particular, polymeric chains with differing chain lengths [16, 50] is considered. Mixed-chain systems show a highly nonlinear change of the bending modulus from the values of the pure systems because the longer chains can take advantage of the free volume in the region near the short chains. The effective modulus and spontaneous curvature of mixed systems have important implications for possible phase separations and even the stabilization of equilibrium vesicles with different compositions in each leaflet of the bilayer [51, 52].

### 6.1. Thermal fluctuations of thin films

The long-wavelength fluctuations of interfaces and membranes have been shown to reduce the effective bending energy. The physical origin of this effect is that the interface spontaneously undergoes a certain amount of bending owing to the increased entropy of the disordered structure; to what extent this occurs is of course a balance of the bending energy and the thermal forces. Thus, for any given bend imposed on the system, there is some probability that the interface will be spontaneously bent in a somewhat similar configuration due to the thermal

fluctuations. Entropy thus increases the probability of spontaneous bends and can be thought of as effectively reducing the bending energy.

Theoretical treatments of this effect were first presented in [1, 47] and have also been recently studied using computer simulations [53]. Here we present a simple derivation of the effective reduction of the bending energy due to the long-wavelength fluctuations which yields the renormalization obtained by most investigators.

For simplicity we consider the case of zero spontaneous curvature where the bending energy is the integral of the square of the curvature over the entire surface. We use the expression for the curvature in the Monge gauge (equation (2.10)) where the surface is described by the local height  $h(x, y)$  above a reference plane. When the interface is nearly flat, the terms  $h_x = \partial h / \partial x$  and  $h_y$ , proportional to the local slopes can be neglected and the mean curvature is proportional to  $h_{xx} + h_{yy}$ . Similarly, terms in the derivatives of  $h$  which appear in the local area element can be neglected. The bending energy is then quadratic in the second derivatives of the local height and the bending energy  $F_b$  is harmonic when calculated as a function of the Fourier transform:

$$h_q = \frac{1}{L^{1/2}} \int d\mathbf{r} h(\mathbf{r}) \exp [i(\mathbf{q} \cdot \mathbf{r})], \quad (6.1)$$

$$F_b = \frac{k}{2} \sum_q q^4 |h_q|^2, \quad (6.2)$$

where  $\mathbf{r} = (x, y)$  and  $L$  is the system size. To be consistent with the rest of the literature, we write the bending energy per unit area as  $f_b = 2kH^2$ , where  $H$  is the mean curvature, related to the height  $h(x, y)$  by equation (2.12). Thus, when considering the degrees of freedom which are the Fourier modes, one has a harmonic energy with a cost  $kq^4/2$ , per mode, where  $k$  is the bare bending constant.

On the other hand, as the interface begins to wander further and further from the reference plane, the finite slope cannot be neglected; this is most important at long length scales where the cost of making a relatively large-angle bend is reduced since the bend is spread out over a large distance. As the energy cost is reduced, the probability that such a bend will occur in thermal equilibrium increases and one must include the terms proportional to  $h_x$  and  $h_y$ . A simple approximation is to write the complete bending energy, using equation (2.10) where the terms proportional to  $h_x^2$ ,  $h_y^2$  and  $h_x h_y$  are replaced by their mean values calculated for the nearly flat membrane. This gives the first perturbation to the harmonic energy. The mean curvature is thus approximated as:

$$H = \frac{(1 + \eta)h_{yy} + (1 + \eta)h_{xx}}{2(1 + \eta + \eta)^{3/2}}, \quad (6.3)$$

where  $\eta = \langle h_x^2 \rangle = \langle h_y^2 \rangle$  and  $\langle h_x h_y \rangle = 0$ . Within the harmonic approximation

$$\eta = \langle h_x^2 \rangle = \frac{k_B T}{4\pi k} \int dq \frac{1}{q} = \frac{k_B T}{4\pi k} \log \left( \frac{L}{a} \right), \quad (6.4)$$

where the high- $q$  cut-off is proportional to the inverse of the molecular size  $a$ , and the low- $q$  cut-off is proportional to the inverse of the system size  $L$ .

Since this is a perturbative approach ( $\eta$  is calculated using the probability factor of the nearly flat membrane), to be consistent, one must expand the mean curvature to first order in  $\eta$  and one finds for the square of the mean curvature

$$H^2 \approx \frac{1}{4}(h_{xx} + h_{yy})^2(1 - 4\eta). \quad (6.5)$$

To find the total bending energy, one integrates  $H^2$  over the surface, approximating the local area element  $(1 + h_x^2 + h_y^2)^{1/2}$  by  $1 + \eta$ . The net result is that the bending energy is written as

$$F_b \approx \frac{k}{2} \left[ 1 - 3 \frac{k_B T}{4\pi\kappa} \log\left(\frac{L}{a}\right) \right] \int \mathrm{d}\mathbf{r} (h_{xx} + h_{yy})^2. \quad (6.6)$$

This has the same form as the bending energy of the nearly flat membrane but with a renormalized and softened bending modulus:

$$k_r = k \left[ 1 - 3 \frac{k_B T}{4\pi\kappa} \log\left(\frac{L}{a}\right) \right]. \quad (6.7)$$

Thus, the long-wavelength undulations of the interface effectively soften the energy to bend the interface in a manner that increases logarithmically with the system size. One can identify the system size at which this approximation for the effective bending modulus yields no cost for bends ( $k_r = 0$ ). This determines the persistence length  $L^* = a \exp(4\pi\kappa/3k_B T)$  at which there is a relatively high probability that the interface will spontaneously bend owing to its fluctuations.

Similar considerations can be used to estimate the renormalization of the Gaussian curvature modulus and the spontaneous curvature [46]. The Gaussian modulus, which in almost all microscopic models is negative (thus favouring spherical structures as opposed to saddles) becomes more positive (thus favouring more saddle-shaped structures) owing to the effect of the thermal undulations. The spontaneous curvature increases with the fluctuations since they tend to ripple the interface further in the direction in which it spontaneously prefers to bend.

## 6.2. Amphiphilic mixtures: interactions and chain mixing

Mixtures of amphiphiles can provide a way of tailoring the microstructure of self-assembled systems by simple composition variations. In addition, the phase diagrams of mixed systems have been shown to be qualitatively different from those expected by a simple average of the components; for example, mixtures of surfactants can form thermodynamically stable vesicles [51] for systems where each of the separate components form only micelles. Mean-field models of mixed surfactant systems have been discussed in [16, 54, 55] where it is shown that the effective bending modulus of a mixed system is not a simple compositional average of the moduli of each species. It is found that the addition of small amounts of short chains to an interface composed mainly of long-chain molecules can have a dramatic effect (nonlinear in the fraction of short chains) on the softening of the bending modulus. The physical reason for this is that the long chains adjacent to the short chains can make very efficient entropic use of the free volume in the region above the short chains and this has a relatively strong effect on lowering the bending stiffness of the system.

Analytic insight into this phenomenon can be obtained by considering a model of either grafted or block copolymers at an interface. In the case of irreversibly grafted



chains (where the area per chain is fixed by the grafting process) several groups [15, 50, 56] have determined the dependence of the free energy and the curvature moduli on the composition. As discussed above, for a single chain length, in this case of non-equilibrated chain packing, the bending modulus scales as  $N^3$  where  $N$  is the polymerization index. The dependence on the composition indicates that indeed, when the volume fraction  $\phi_l$  of long chains is small, the modulus is hardly affected and

$$k \sim N_s^3 \left( 1 + \frac{16\alpha\phi_l^3}{3} + \dots \right), \quad (6.8)$$

where  $N_s$  is the degree of polymerization of the short chains and  $\alpha = (N_\ell - N_s)/N_s$  is a measure of the molecular weight difference between the long and short chains. On the other hand, the addition of a small amount of short chains has a more dramatic effect on the bending modulus of a brush composed of mostly long chains and for  $\phi_\ell \approx 1$

$$k \sim N_\ell^3 \left( 1 - \frac{5\alpha(1 - \phi_l)}{(1 + \alpha)} + \dots \right). \quad (6.9)$$

Of course, if the chains can equilibrate their packing areas, the area per chain depends somewhat on the curvature and the bending moduli are further reduced as in the case of the single-component system [50]. However, the effects of mixing a small number of long chains in a layer of mostly short chains is much less dramatic than the mixing of a small number of short chains in a layer of mostly long chains as discussed above.

## 7. Experimental measurements of curvature elasticity

In this section, we briefly review several experimental tests of the influence of the curvature energy on the properties of microemulsions and vesicles. While microemulsions exhibit a wide variety of interesting morphologies and phases, the simplest case is where the domains are spherical and the system can be modelled as consisting of a nearly monodisperse set of spherical droplets. This picture is applicable to systems with relatively large spontaneous curvatures of the monolayer and large bending moduli. Since the structure is simple in these cases, one can study these systems more quantitatively to see whether the properties reflect in an unambiguous way the determining influence of the curvature energy. Here we present an example whereby the scaling of experimentally measurable quantities with drop size provide strong evidence for the relevance of the bending energy (and not the stretching energy) to large-scale microemulsions. We then mention some experiments on bilayer vesicle systems and conclude with some recent results which attempt to determine the dependence of the bending modulus on the electrostatics of the polar head groups and their associated counterions.

### 7.1. Experimental estimates of bending moduli

We begin with the monolayer films found in microemulsions. Measurements and analysis of the dynamical fluctuations of microemulsion drops provide information on the restoring forces which resist these fluctuations and hence on the bending energy [57–59]. The reader is referred to the references for the details; here we merely mention that the scaling of the characteristic time scale with the drop size can differentiate between restoring forces which arise from bending energy and those

which arise from an actual stretching or compression of the surfactant interface. The microemulsion experiments referred to above show that the slowest time scales are those associated with bending fluctuations.

In bilayer systems, there have been many experimental attempts to estimate bending moduli of isolated globules such as vesicles, mostly by analysis of the amplitude of the thermal fluctuations of the vesicle; a comprehensive and critical survey of these experimental results is outside the scope of this paper. For reviews see [3, 60] and the references therein. Of particular note are experiments using micropipette pressure [61] and optical techniques [62]. The spontaneous curvature of lipid–water systems has been studied in [63].

Finally, we note that the scaling of the bending constants with the chain length has been estimated in recent experiments [34]. Increasing the chain length of the surfactants from  $C_8$  to  $C_{10}$  results in an increase in the elastic constant by a factor of two, while an increase from  $C_8$  to  $C_{12}$  results in an increase of 3.6 in the elastic constant. These very nonlinear dependences of the bending moduli on the chain length are at least qualitatively consistent with the predictions discussed above.

### 7.2. Emulsification failure: drop size and interfacial tension

While the presence of a spherical phase of droplets cannot by itself either prove or disprove the dominance of the bending energy in determining the properties of microemulsions, the transitions from a single-phase to multiphase coexistence can be an important indicator. Neglecting fluctuations in the droplet size and shape, conservation of the internal phase (to be specific we shall assume it is oil) and the surfactant with volume fractions  $\phi_o$  and  $\phi_s$ , respectively, imply that the radius of the spherical droplets is given by  $R = 3\delta\phi_o/\phi_s$ , where  $\delta$  is a typical surfactant size. This conservation law neglects changes in the area per molecule with curvature which give higher-order corrections to this law (of order  $\delta/R$ ); the observation of a nearly linear increase in the drop size with increasing ratio  $\phi_o/\phi_s$  is one indication of the fact that the area per molecule is nearly equal to its value in the flat film. Naturally, this approximation breaks down when  $R/\delta$  becomes of order unity but, as mentioned at the outset, we focus on the properties of microemulsions with large domain sizes compared with molecular scales.

For a phase of spherical droplets, the conservation laws determine the actual drop size, while the bending energy determines the optimal droplet size. Minimization of equation (1.1) with respect to the curvature indicates that the optimal drop size  $R^*$  is proportional to  $c_0^{-1}$ ; the spontaneous curvature sets the drop size which minimizes the bending free energy. Thus, if  $R < R^*$ , the system has no choice but to keep a uniform phase of spherical droplets (when  $R$  differs significantly from  $R^*$ , other shapes are possible [2]) but, when  $R > R^*$ , the droplets cease to grow and expel the excess inner phase (e.g. the oil) into a coexisting phase. This has been termed an emulsification failure instability [64] (figure 10). The simple picture described here is somewhat modified by contributions coming from the fluctuations of the droplet shape, the entropy of mixing, and possible (weak) interactions between the droplets, but in the limit of large bending moduli ( $k \gg k_B T$ ) our approximations are appropriate.

Thus, the bending energy predicts a maximum drop size with a two-phase equilibrium with the excess internal phase. On the triangular phase diagram, this phase boundary which occurs when  $R \sim \phi_o/\phi_s \sim c_0^{-1}$  should be a straight line. The droplet size at emulsification failure is a measure of the spontaneous curvature.

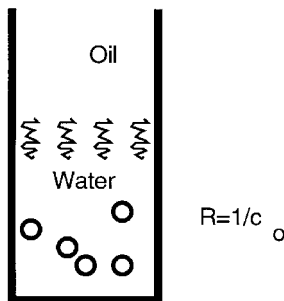


Figure 10. Emulsification failure in a microemulsion. The droplets of oil in water are at their spontaneous curvature. The macroscopically flat interface between the water containing the microemulsion and the phase of excess oil is covered by a surfactant monolayer whose tension is discussed in the text.

Measurements of the drop size along the phase boundary for the coexistence of nearly spherical microemulsion drops with excess internal phase (oil) in non-ionic systems [65] indicates that the spontaneous curvature varies linearly with temperature in this regime. For these systems, it appears that corrections to the linear phase boundary due to entropy of mixing effects are small.

The observation of such a straight-line phase boundary is therefore an indication of the validity of this picture. A consistency check consists of measurements of the interfacial tension between the microemulsion (in our example, oil in water) of optimal droplets and the excess phase (water, in our example). This interface consists of a monolayer of surfactant and the tension is just the energy to make more flat interface from the preferred droplets that is, the bending energy cost of a flat interface in a system with a strong spontaneous curvature. This energy cost per unit length is just proportional to the inverse drop size squared. Thus measurements of the tension as a function of droplet size are predicted to have an inverse square relationship due to the bending energy.

Recent experiments [34, 66] using both scattering techniques and interfacial tension measurements have shown that a variety of microemulsion-forming non-ionic surfactants obey the scaling relationship  $\gamma \sim 1/R^2$ . In addition, the bending moduli extracted [34] from the dependence of this relationship on  $k$  and  $k$  is consistent with the moduli deduced from analysis of the neutron scattering spectra for fluctuating microemulsion droplets.

### 7.3. Electrostatic contributions to the bending modulus

In a recent paper [67], it is shown that the bending constant can be estimated experimentally from experiments which determine the interlayer distance in a lamellar phase of an oil–water–surfactant microemulsion. Fluctuation corrections to the conservation of surfactant area due to the thermal crumpling of the surfactant layers result in a correction to the swelling law for the smectic period  $d$  and one expects that

$$d = \frac{\delta}{\phi_s} (A - B \log \phi_s), \quad (7.1)$$

where  $\phi_s$  is the surfactant volume fraction,  $\delta$  is the surfactant layer thickness, and  $A$  and  $B$  are coefficients that are functions of the bending constant  $k/k_B T$ . By careful

fitting of the X-ray measurements of the periodicity of these lamellar systems, one can estimate the bending modulus  $k$ .

For charged surfactant with no added salt, the bending modulus was deduced from the measurements as a function of the increasing thickness of the water layer. According to the theory outlined above, the modulus  $k$  should increase linearly with increasing water region thickness owing to the long-range nature of the electrostatic interactions. What was observed, however, was that  $k$  initially decreased with increasing water thickness and then at a thickness of about 15 Å saturated at a value of about  $0.3k_B T$ . The predicted increase was certainly not observed. Freyssingeas *et al.* [67] attributed this striking discrepancy between theory and experiment to the possibility that the numerical pre-factor relating  $k$  and the water thickness may be quite small (of the order of  $0.14k_B T \text{ Å}^{-1}$ ) and that this causes the electrostatic contribution to  $k$  to be undetectable with the present experiment. However, it is strange that such a strong dependence of  $k$  on water thickness should not be observable at least at very large thicknesses and further inquiry may be useful.

### Acknowledgments

The author is grateful to the collaborators, colleagues and students whose work is included here and in the references below including N. Dan, D. Srolovitz, T. Tlusty, and Z.-G. Wang. R. Menes and T. Tlusty offered many valuable comments on this manuscript and the author acknowledges their help. This research was supported by the Donors of the Petroleum Research Fund, the Israel Academy of Arts and Sciences, and the Israel–French collaborative program supported by the Israel Ministry of Science.

### References

- [1] GELBART, W., BEN SHAUL, A., and ROUX, D. (editors), 1994, *Micelles, Membranes, Microemulsions and Monolayers* (New York: Springer).
- [2] SAFRAN, S. A., 1994, *Statistical Thermodynamics of Surfaces, Interfaces, and Membranes* (Reading, Massachusetts: Addison-Wesley).
- [3] LIPOWSKY, R., and SACKMANN, E. (editors), 1995, *Structure and Dynamics of Membranes* (Amsterdam: North-Holland).
- [4] GOMPPER, G., and SCHICK, M., 1994, *Self-Assembling Amphiphilic Systems* (New York: Academic Press).
- [5] KROTO, H. W., 1992, *Angew. Chem.*, **31**, 111.
- [6] IJIMAA, S., 1991, *Nature*, **354**, 56.
- [7] MACKAY, A. L., and TERRONES, H., 1991, *Nature*, **352**, 762 (1991); D. VANDERBILT, and J. TERSOFF, 1992, *Phys. Rev. Lett.*, **68**, 511; T. LENOSKY, X. GONZE, M. TETER, and V. ELSEER, 1992, *Nature*, **355**, 333.
- [8] HELFRICH, W., 1973, *Z. Naturf. (c)* **28**, 693; P. B. CANHAM, 1970, *J. theor. Biol.*, **26**, 61.
- [9] SUEZAKI, Y., and ICHINOSE, H., 1995, *J. Phys., Paris*, **I**, **5**, 1469.
- [10] WANG, Z.-G., and SAFRAN, S. A., 1990, *J. Phys., Paris*, **51**, 185.
- [11] ANDELMAN, D., 1995, In *Structure and Dynamics of Membranes*, edited by R. Lipowsky and E. Sackmann (Amsterdam: North-Holland), p. 607.
- [12] PINCUS, P., JOANNY, J., and ANDELMAN, D., 1990, *Europhys. Letts.*, **11**, 763.
- [13] HIGGS, P., and JOANNY, J., 1990, *J. Phys., Paris*, **51**, 2307.
- [14] LEKERKERKER, H., 1989, *Physica A*, **159**, 319.
- [15] ALEXANDER, S., 1977, *J. Phys., Paris*, **38**, 983; Milner, S., WITTEN, T., and CATES, M., 1988, *Macromolecules*, **21**, 2610; Skvostov, A. M., *et al.*, 1988, *Vysokomol. Soedin. A*, **30**, 1615.

- [16] SZLEIFER, I., KRAMER, D., BEN SHAUL, A., GELBART, W. H., and SAFRAN, S. A., 1990, *J. Chem. Phys.*, **92**, 6800; GELBART, W., BEN SHAUL, A., and ROUX, D. (editors), 1994, *Micelles, Membranes, Microemulsions and Monolayers* (New York: Springer), Chapter 1.
- [17] DAN, N., and SAFRAN, S. A., 1994, *Macromolecules*, **27**, 5766; 1973, *Europhys. Lett.*, **21**, 975.
- [18] ROMERO-ROCHIN, V., VAREA, C., ROBLEDO, A., 1991, *Phys. Rev. A*, **44**, 8417; 1993, *Phys. Rev. E*, **46**, 1600; GOMPPER, G., and ZSCHOCKE, S., 1991, *Europhys. Lett.*, **18**, 731; BLOCKHUS, E. M., and BEDEAUX, D., 1993, *Molec. Phys.*, **80**, 705.
- [19] LANDAU, L. D., and LIFSHITZ, E. M., 1986, *Theory of Elasticity*, third edition (Oxford: Pergamon).
- [20] HELFRICH, W., 1981, *Physics of Defects*, Les Houches, Section XXXV, edited by R. Balian, M. Kleman and J. P. Poirier (Amsterdam: North-Holland), p. 713.
- [21] SROLOVITZ, D. J., SAFRAN, S. A., and TENNE, R., 1994, *Phys. Rev. E*, **49**, 5260.
- [22] TERSOFF, J., 1997, *Phys. Rev. B*, **46**, 15 546.
- [23] LOVE, A. E. H., 1892, *A Treatise on the Mathematical Theory of Elasticity*, Vol. I (Cambridge University Press).
- [24] HIRTH, J. P., and LOTHE, J., 1982, *Theory of Dislocations*, second edition (New York: Wiley).
- [25] NYE, J. F., 1949, *Proc. R. Soc. A*, **200**, 47.
- [26] READ, W. T., 1957, *Acta metall.*, **5**, 83.
- [27] WEERTMAN, J., and WEERTMAN, J. R., 1964, *Elementary Dislocation Theory* (London: Macmillan).
- [28] FRANK, F. C., and VAN DER MERWE, J. H., 1949, *Proc. R. Soc. A*, **198**, 216.
- [29] SROLOVITZ, D. J., SAFRAN, S. A., TENNE, R., and HOMYONFER, M., 1995, *Phys. Rev. Letts.*, **74**, 1779.
- [30] KÓZLOV, M. M., LEIKIN, S. L., and MARKIN, V. S., 1985, *J. chem. Soc., Faraday Trans.*, **2**, 277.
- [31] BLAKESLEE, O. L., PROCTOR, D. G., SELDIN, E. J., SPENCE, G. B., and WENG, T., 1970, *J. appl. Phys.*, **41**, 3373.
- [32] FOREMAN, A. J. E., 1955, *Acta metall.*, **3**, 322.
- [33] PETROV, A. G., and BIVAS, 1984, *Prog. Surf. Sci.*, **16**, 389.
- [34] GRADZIELSKI, M., LANGEVIN, D., and FARAGO, B., 1996, *Phys. Rev. E*, **53**, 3900; GRADZIELSKI, M., HOFFMANN, H., and LANGEVIN, D., 1995, *J. phys. Chem.*, **99**, 12 612.
- [35] SAFRAN, S. A., PINCUS, P. A., CATES, M. E., and MACKINTOSH, F. C., 1990, *J. Phys., Paris*, **51**, 503.
- [36] ALEXANDER, S., CHAIKIN, P. M., GRANT, P., MORALES, G. J., PINCUS, P., and HONE, D., 1984, *J. chem. Phys.*, **80**, 5776.
- [37] CANTOR, R. S., 1981, *Macromolecules*, **14**, 1186.
- [38] WANG, Z.-G., and SAFRAN, S. A., 1991, *J. chem. Phys.*, **94**, 679.
- [39] LEIBLER, L., 1988, *Makromol. Chem., Macromol. Symp.*, **16**, 1.
- [40] DEGENNES, P. G., 1979, *Scaling Concepts in Polymer Physics* (Ithaca, New York: Cornell University Press).
- [41] PINCUS, P., 1989, *Phase Transitions in Soft Condensed Matter*, edited by T. Riste and D. Sherrington (New York: Plenum).
- [42] MILNER, S. T., and WITTEN, T. A., 1988, *J. phys., Paris*, **49**, 1951.
- [43] LEIBLER, S., and ANDELMAN, D., 1987, *J. Phys., Paris*, **48**, 2013.
- [44] FOURNIER, J. B., 1996, *Phys. Rev. Lett.*, **76**, 4436.
- [45] ANDELMAN, D., CATES, M., ROUX, D., and SAFRAN, S. A., 1987, *J. chem. Phys.*, **87**, 7229.
- [46] PALMER, K., and MORSE, D. C., 1996, *J. chem. Phys.*, **105**, 11147.
- [47] HELFRICH, W., 1985, *J. Phys., Paris*, **46**, 1263; PELITI, L., and LEIBLER, S., 1985, *Phys. Rev. Lett.*, **54**, 1690.
- [48] MORSE, D. C., and MILNER, S. T., 1994, *Europhys. Lett.*, **26**, 565.
- [49] PETROV, A. G., BOLTENHAGEN, P., and KLEMAN, M., unpublished.
- [50] MILNER, S. T., WITTEN, T. A., and CATES, M. E., 1989, *Macromolecules*, **22**, 853; DAN, N., and SAFRAN, S. A., 1994, *Macromolecules*, **27**, 5766.
- [51] KALER, E. W., MURTHY, A. K., RODRIGUEZ, B. E., and ZASADZINSKI, J. A. N., 1989, *Science*, **245**, 1371.

- [52] SAFRAN, S. A., PINCUS, P. A., and ANDELMAN, D., 1990, *Science*, **248**, 354; SAFRAN, S. A., PINCUS, P. A., ANDELMAN, D., and MACKINTOSH, F. C., 1991, *Phys. Rev. A*, **43**, 1071.
- [53] GOMPPER, G., and KROLL, D. M., 1996, *J. Phys., Paris I*, **6**, 1397.
- [54] MAY, S., and BEN-SHAUL, A., 1995, *J. chem. Phys.*, **103**, 3839; BEN-SHAUL, A., 1995, *Handbook of Biological Physics*, edited by R. Lipowsky and E. Sackmann (Amsterdam: Elsevier Science), p. 359.
- [55] KOZLOV, M. M., and HELFRICH, W., 1992, *Langmuir*, **8**, 2792.
- [56] BIRSHTEIN, T. M., LIATSKAYA, YU., V., and ZHULINA, E. B., 1990, *Polymer*, **31**, 2185.
- [57] SAFRAN, S. A., 1983, *J. chem. Phys.*, **78**, 2073; BORKOVIC, N., 1992, *Adv. Colloid Interface Sci.*, **31**, 195.
- [58] MILNER, S. T., and SAFRAN, S. A., 1987, *Phys. Rev. A*, **36**, 4371.
- [59] HUANG, J. S., MILNER, S. T., FARAGO, B., and RICHTER, D., 1987, *Phys. Rev. Lett.*, **59**, 2600; FARAGO, B., HUANG, J. S., RICHTER, D., SAFRAN, S. A., and MILNER, S. T., 1990, *Phys. Rev. Lett.*, **65**, 3348.
- [60] SACKMANN, E., 1994, *FEBS Lett.*, **346**, 3.
- [61] EVANS, E. A., and WAUGH, R., 1981, *Biophys. J.*, **54**, 495.
- [62] DUEW, H., and SACKMANN, E., 1990, *Physica A*, **163**, 410.
- [63] GRUNER, S., PARSEGIAN, A., and RAND, P., 1980, *Faraday Discuss. chem. Soc.*, **81**, 267.
- [64] SAFRAN, S. A., and TURKEVICH, L. A., 1983, *Phys. Rev. Lett.*, **50**, 1930.
- [65] LEAVER, M. S., OLSSON, U., WENNERSTROM, H., and STREY, R., 1995, *J. chem. Soc., Faraday Trans.*, **91**, 4269.
- [66] STREY, R., 1994, *Colloid Polym Sci.*, **272**, 1005.
- [67] FREYSSINGEAS, E., ROUX, D., and NALLET, F., 1996, *J. Phys., condens. Matter*, **8**, 2801.